EUROPEAN JOURNAL OF PURE AND APPLIED MATHEMATICS
2025, Vol. 18, Issue 3, Article Number 6423
ISSN 1307-5543 – ejpam.com
Published by New York Business Global

A Spatiotemporal Framework for Malaria Control Integrating Exposure Heterogeneity and Optimal Strategy Deployment

Nadeem Abbas[1], Wasfi Shatanawi[1,2], Syeda Alishwa Zanib[3,*]

[1] *Department of Mathematics and Sciences, College of Humanities and Sciences, Prince Sultan University, Riyadh, 11586, Saudi Arabia*
[2] *Department of Mathematics, Faculty of Science, The Hashemite University, P.O Box 330127, Zarqa 13133, Jordan*
[3] *Department of Mathematics, Riphah International University, Main Satyana Road, Faisalabad 44000, Pakistan*

Abstract. Malaria remains one of the most serious and widespread vector-borne infectious diseases worldwide, caused by *Plasmodium* protozoa and transmitted through the bites of infected female Anopheles mosquitoes. In this study, we present a novel, integrative, bioinformatics-driven deterministic mathematical model to investigate the complex transmission dynamics of malaria. The model uniquely distinguishes between homogeneous and heterogeneous exposed human compartments (E_{hm}, E_{ht}) and explicitly incorporates mosquito population dynamics. The coupled system includes human compartments S_M, E_{hm}, E_{ht}, I_M, H_M, R_M, and mosquito compartments S_F, E_F, I_F. We perform a comprehensive stability analysis of both the malaria-free and endemic equilibrium points, assessing global stability in relation to the basic reproduction number R_0. Sensitivity analysis reveals that the mosquito biting rate (α_M) and the transmission probability (β_M) are key parameters influencing malaria spread. To evaluate the effectiveness of intervention strategies, we incorporate time-dependent control variables and formulate an optimal control problem using Pontryagin's Maximum Principle. The control interventions include bed net usage (m_1), antimalarial medication treatment (m_2), and insecticide spraying (m_3). Numerical simulations, implemented using a fourth-order Runge-Kutta method in `Python` and `MATLAB`, demonstrate the significant impact of these strategies in reducing both exposed and infected populations. Our findings emphasize the importance of timely and targeted control measures and highlight the effectiveness of integrating bioinformatics with mathematical modeling to support informed decision-making in malaria control policies.

2020 Mathematics Subject Classifications: 26A33, 34A08, 03C65

Key Words and Phrases: Malaria Disease, Mathematical Model, Optimal Control, Homogeneous and Heterogeneous Individuals, Sensitivity Analysis

1. Introduction

One of the most serious infectious diseases in the world is malaria, a potentially fatal vector-borne disease spread by the protozoan Plasmodium that infects female Anopheles mosquitoes and bites

*Corresponding author.
DOI: https://doi.org/10.29020/nybg.ejpam.v18i3.6423
Email addresses: `nabbas@psu.edu.sa` (N. Abbas), `wshatanawi@psu.edu.sa` (W. Shatanawi),`19907@riphahfsd.edu.pk` (S. A. Zanib)

people [1–5]. The causative agents, including Plasmodium falciparum, Plasmodium vivax, Plasmodium ovale, and Plasmodium malariae, exhibit differences in microscopic appearance, geographical distribution, and clinical characteristics, particularly in terms of infection potential, severity, and propensity for relapse shown in Figure 1. Among them, P. falciparum is recognized as the most perilous to humans [6]. Malaria is spread from person to person by mosquito bites. Plasmodium vivax and P. falciparum are the two most common malaria species that infect people among the five species that affect malaria overall. More than 400,000 deaths a year are caused by these two species, with 90% of the deaths occurring in Africa.

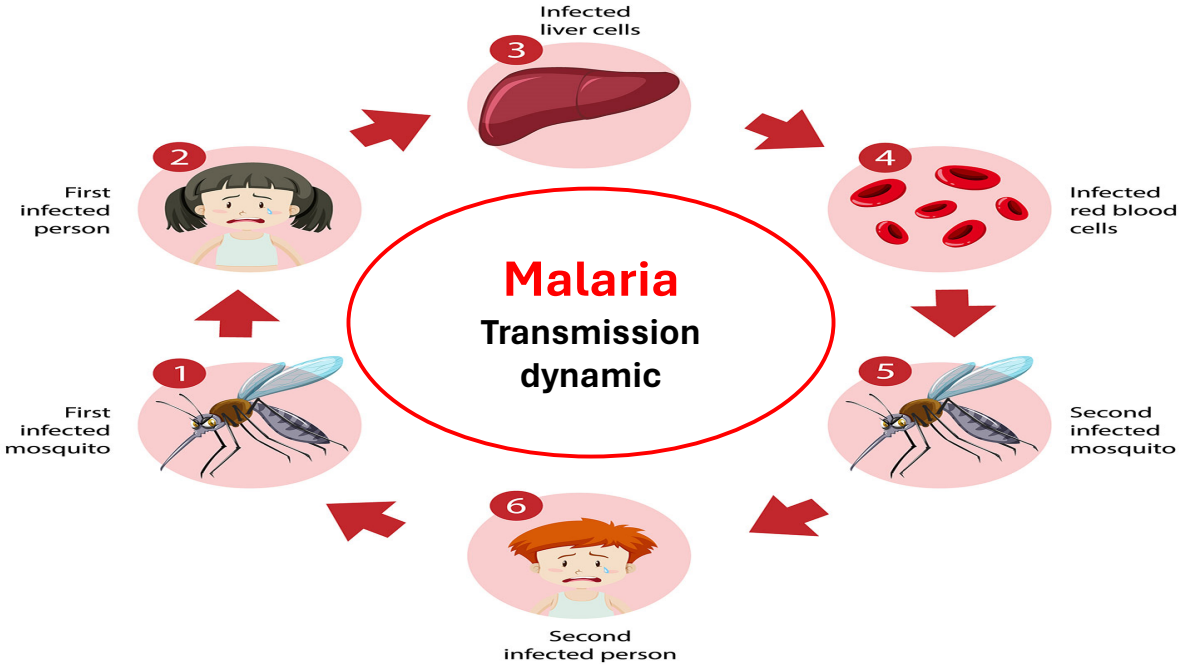

Figure 1: *Malaria Transmission*

According to the latest World Malaria Report of December 2019, there were 228 million reported cases of malaria in 2018, a slight decline from 231 million cases in 2017. In 2018, an estimated 405,000 people succumbed to the disease, compared to 416,000 in 2017. The burden of malaria remains disproportionately high in the WHO African Region, accounting for 93 % of cases and 94% of deaths in 2018. Malaria prevalence spans over 100 countries, resulting in approximately 216 million cases and 655,000 deaths in 2010 [7, 8]. Despite longstanding efforts to combat malaria, it persists as a major public health challenge in affected areas, primarily in tropical and subtropical regions of Africa, the Eastern Mediterranean, Asia, and South America. Vulnerable populations include pregnant women and non-immune travelers. Beyond its health-related implications, malaria poses a significant socioeconomic threat to endemic nations. In Africa alone, the annual economic burden of malaria was estimated at 8 billion [2, 5, 9]. Consequently, there has been a critical need to devise various intervention strategies to mitigate the impact of malaria. While global efforts are underway to develop a perfect vaccine against malaria, none currently exists [5, 10–16]. To control the spread of the disease, preventive measures include mosquito-reduction strategies

and personal protection against mosquito bites, facilitated by the use of insecticide-treated bed nets (ITNs), intermittent preventive treatment (IPT), and the elimination of vector breeding sites [2, 17–19]. Additional intervention strategies encompass indoor residual spraying (IRS) to eliminate infected indoor mosquitoes and the sterile insect technique. The use of anti-malarial drugs also plays a role in regulating malaria [6, 20–23]. Numerous mathematical models have been developed to investigate fluid dynamics, neurological processes, and the transmission dynamics of epidemic diseases over time [24–32]. Oke et al. (2020)[20] studied the malaria dynamics transmission using a non-linear mathematical model. He studied stability theory, optimum control techniques and numerical simulations to show how different control strategies affect the spread of disease. Tchoumi et al., (2021) [33] investigated the co-dynamics of malaria and COVID-19 in order to determine the best control techniques and stability conditions. Results indicated that treating both infections at the same time prevented their spread more successfully, which shed light on the difficulties encountered during the COVID-19 pandemic. In sense of fractional derivatives , Sinan et al., (2022) [34] used and non-linear mathematical model to study the malaria dynamics spread by mosquito vectors. The effectiveness of control measures like bed nets and pesticides in the spread of infections was demonstrated using numerical simulations. Alhaj (2023) [35] studied a deterministic model for Malaria transmission, analyzing the basic reproduction number (R0) and stability conditions. Simulation and sensitivity analysis highlight control interventions' impact, providing recommendations for eradicating Malaria transmission. Adegbite et al. (2023)[36] explored malaria importation's impact globally, using a novel ODEs system to evaluate vigilance-driven conventional and traditional control strategies, emphasizing the need for 98% vigilance for effective malaria management. Alqahtani et al, (2024) [37] modeled using a deterministic fractional-order system incorporating a novel hospitalized compartment to simulate transmission dynamics between humans and mosquitoes. The basic reproduction number was derived using the next-generation matrix method, and numerical simulations were performed using the fourth-order Runge–Kutta method in MAPLE. Olutimo et al., (2024) [38] explored the influence of environmental immunity on malaria transmission through a developed SIR-SI mathematical model. The analysis revealed that the malaria-free equilibrium was locally asymptotically stable when the reproduction number was below unity. Numerical simulations demonstrated that acquired environmental immunity, influenced by nutrition and medicinal herbs, significantly diminished malaria spread by bolstering the recovered class and reducing the infected class. This paper presents a dynamic mathematical model to investigate malaria transmission dynamics, building upon earlier studies. Our primary goal is to identify and assess effective control strategies for disease management. To this end, we develop an optimal control model that incorporates interventions such as treated bed nets, pesticide application, hospitalization, and preventive treatment. A novel aspect of our research is the division of the exposed human population into two distinct classes based on genetic heterogeneity: homogeneous and heterogeneous individuals, reflecting differences in resistance to malaria. The genetic basis of hemoglobin variants, particularly the sickle cell allele, is highly prevalent in African populations, where malaria transmission is also endemic. heterogeneous individuals carrying the sickle cell trait exhibit increased resistance to *Plasmodium falciparum* infection and often remain asymptomatic despite exposure, whereas homogeneous individuals are more susceptible to infection and disease symptoms [39]. Additionally, our model introduces a hospitalized class, which is a novel variable rarely considered in malaria modeling literature. This inclusion allows us to better capture the dynamics of severe cases and healthcare interventions. To determine the optimal control strategies, we apply Pontryagin's Maximum Principle (PMP), a powerful tool in optimal control theory.

Furthermore, we calculate the basic reproduction number R_0 and perform sensitivity analysis to evaluate the influence of key parameters on disease transmission and control efficacy. This model serves as a valuable framework for evaluating the effectiveness of various malaria control measures and enhances understanding of malaria dynamics post-intervention within populations.

2. Model Analysis

We develop an $S_M E_{hm} E_{ht} I_M H_M R_M$–$S_F E_F I_F$ compartmental model to simulate malaria transmission dynamics between humans and mosquitoes. The human population is structured into six distinct compartments: susceptible individuals (S_M), heterogeneously exposed individuals (E_{ht}), homogeneously exposed individuals (E_{hm}), infected individuals (I_M), hospitalized individuals (H_M), and recovered individuals (R_M). Recovered individuals acquire temporary immunity but eventually re-enter the susceptible compartment (S_M) due to waning immunity. The mosquito population (female Anopheles) is categorized into three compartments: susceptible mosquitoes (S_F), exposed mosquitoes (E_F), and infectious mosquitoes (I_F). Crucially, both infected and recovered humans transmit the malaria parasite to mosquitoes during blood-feeding events, as illustrated in the transmission flowchart (Figure 2). The total human population at time t is given by:

$$T_M = S_M + E_{hm} + E_{ht} + I_M + H_M + R_M, \tag{2.1}$$

while the total mosquito population is:

$$T_F = S_F + E_F + I_F. \tag{2.2}$$

The parameters governing the model are systematically defined in Table 1. The mosquito lifecycle is explicitly modeled through three developmental stages: immature/susceptible (S_F), exposed (E_F), and infected (I_F). The resulting malaria transmission dynamics are captured by a coupled system of nonlinear ordinary differential equations:

$$\frac{dS_M}{dt} = \lambda_M - \frac{\alpha_M \, \beta_M \, S_M \, I_F}{T_M} - \epsilon_M \, S_M + \omega_M \, R_M - \gamma_M S_M, \tag{2.3}$$

$$\frac{dE_{hm}}{dt} = \frac{\alpha_M \, \beta_M \, S_M \, I_M}{T_M} - \epsilon_M \, E_{hm} - \varphi_M \, E_{hm}, \tag{2.4}$$

$$\frac{dE_{ht}}{dt} = \gamma_M S_M - (\epsilon_M + \eta_M) \, E_{ht}, \tag{2.5}$$

$$\frac{dI_M}{dt} = \varphi_M \, E_{hm} - (\mu_M + \epsilon_M + \rho_M) \, I_M, \tag{2.6}$$

$$\frac{dH_M}{dt} = \rho_M \, I_M - (\mu_M + \epsilon_M + \delta_M) \, H_M, \tag{2.7}$$

$$\frac{dR_M}{dt} = \eta_M E_{ht} + \delta_M \, H_M - \epsilon_M \, R_M - \omega_M R_M, \tag{2.8}$$

$$\frac{dS_F}{dt} = \lambda_F - \frac{\alpha_M \, \beta_F \, S_F \, I_M}{T_F} + \frac{\alpha_M \, \beta_M \, R_M \, S_F}{T_F} - \epsilon_F \, S_F, \tag{2.9}$$

$$\frac{dE_F}{dt} = \frac{\alpha_M \, \beta_F \, S_F \, I_M}{T_F} + \frac{\alpha_M \, \beta_M \, R_M \, S_F}{T_F} - \phi_M \, E_F - \epsilon_F \, E_F, \tag{2.10}$$

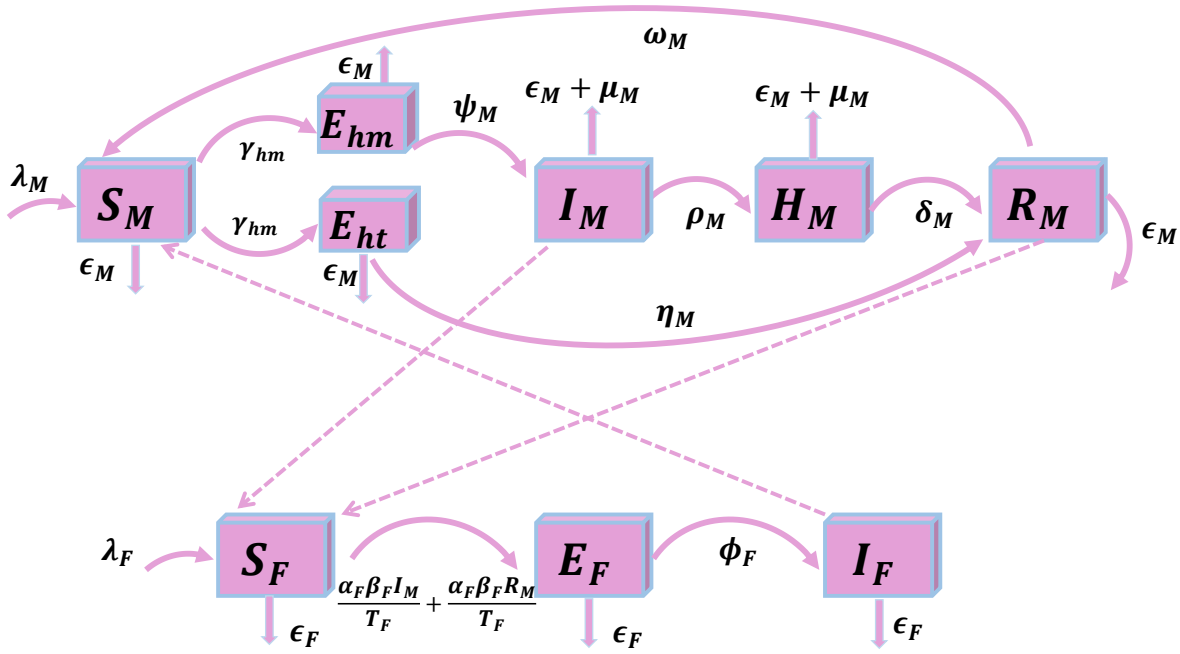

Figure 2: *Schematic representation of malaria transmission dynamics. Solid arrows indicate natural progression; dashed arrows denote infection pathways.*

$$\frac{dI_F}{dt} = -\epsilon_F\, I_F + \phi_M\, E_F, \tag{2.11}$$

having initial conditions,

$$S_M \geq 0, E_{hm} \geq 0, E_{ht} \geq 0, I_M \geq 0, H_M \geq 0, R_M \geq 0, S_F \geq 0, E_F \geq 0, I_F \geq 0. \tag{2.12}$$

2.1. Feasible Region and Positivity of Solutions

Theorem 1. *There exists a feasible region Ω_T in which the solutions of the model (2.3)–(2.11) remain bounded and positively invariant.*

Proof. Summing the equations for the human compartments in system (2.3)–(2.11), we define the total human population as

$$T_M = S_M + E_{hm} + E_{ht} + I_M + H_M + R_M.$$

Differentiating with respect to time yields

$$\frac{dT_M}{dt} = \frac{dS_M}{dt} + \frac{dE_{hm}}{dt} + \frac{dE_{ht}}{dt} + \frac{dI_M}{dt} + \frac{dH_M}{dt} + \frac{dR_M}{dt}.$$

From the model equations, this becomes

$$\frac{dT_M}{dt} = \lambda_M - \epsilon_M(S_M + E_{hm} + E_{ht} + I_M + H_M + R_M) - \mu_M(I_M + H_M).$$

In the absence of disease-induced mortality (i.e., $\mu_M = 0$), the equation simplifies to

$$\frac{dT_M}{dt} = \lambda_M - \epsilon_M T_M.$$

Solving this linear differential inequality gives

$$T_M(t) \leq \left(T_M(0) - \frac{\lambda_M}{\epsilon_M}\right) e^{-\epsilon_M t} + \frac{\lambda_M}{\epsilon_M}.$$

Taking the limit as $t \to \infty$, we have

$$0 \leq T_M(t) \leq \frac{\lambda_M}{\epsilon_M}.$$

Thus, the feasible region for the human population is

$$\Omega_M = \left\{(S_M, E_{hm}, E_{ht}, I_M, H_M, R_M) \in \mathbb{R}^6_+ : S_M + E_{hm} + E_{ht} + I_M + H_M + R_M \leq \frac{\lambda_M}{\epsilon_M}\right\}.$$

Similarly, for the mosquito population, defining

$$T_F = S_F + E_F + I_F,$$

we obtain the feasible region

$$\Omega_F = \left\{(S_F, E_F, I_F) \in \mathbb{R}^3_+ : S_F + E_F + I_F \leq \frac{\lambda_F}{\epsilon_F}\right\}.$$

Therefore, the overall feasible region for the system is

$$\Omega^T = \Omega_M \times \Omega_F,$$

which is positively invariant and bounded.

Theorem 2. *The solutions of the system of equations* (2.3)–(2.11) *with initial conditions* (2) *remain non-negative for all time* $t > 0$.

Proof. Suppose, for the sake of contradiction, that there exists a time $\hat{t} > 0$ such that

$$S_M(\hat{t}) = 0,$$

while for all $t \in (0, \hat{t})$,

$$\begin{aligned} &S_M(t) > 0, \quad E_{hm}(t) > 0, \quad E_{ht}(t) > 0, \quad I_M(t) > 0, \quad H_M(t) > 0, \\ &R_M(t) > 0, \quad S_F(t) > 0, \quad E_F(t) > 0, \quad I_F(t) > 0. \end{aligned}$$

From the system (2.3)–(2.11), the equation for the susceptible human population S_M at time $\hat{t}$ is

$$\left.\frac{dS_M}{dt}\right|_{t=\hat{t}} = \lambda_M - \frac{\alpha_M \beta_M S_M(\hat{t}) I_F(\hat{t})}{T_M} - \epsilon_M S_M(\hat{t}) + \omega_M R_M(\hat{t}) - \gamma_M S_M(\hat{t}).$$

Since $S_M(\hat{t}) = 0$, this reduces to

$$\left.\frac{dS_M}{dt}\right|_{t=\hat{t}} = \lambda_M + \omega_M R_M(\hat{t}) \geq 0,$$

because $\lambda_M > 0$ and $R_M(\hat{t}) \geq 0$. Moreover, for $t \in (0, \hat{t})$, we have

$$\frac{dS_M}{dt} + \epsilon_M S_M(t) \leq \lambda_M + \omega_M R_M(t).$$

Multiplying both sides by the integrating factor $e^{\epsilon_M t}$ and integrating over $[0, \hat{t}]$, we obtain

$$S_M(\hat{t}) \geq S_M(0)e^{-\epsilon_M \hat{t}} > 0,$$

which contradicts the assumption that $S_M(\hat{t}) = 0$. By similar arguments, positivity of the other state variables $E_{hm}, E_{ht}, I_M, H_M, R_M, S_F, E_F, I_F$ can be established for all $t > 0$. Therefore, the solutions remain non-negative for all $t > 0$.

2.2. Malaria-Free Equilibrium Point

The steady state, also known as the malaria-free equilibrium (MFE), is attained when there is no infection present in the population; that is, all exposed and infected compartments are zero. At this equilibrium, the system is at a steady state where the disease does not persist. Setting the derivatives of all compartments to zero,

$$\frac{dS_M}{dt} = \frac{dE_{hm}}{dt} = \frac{dE_{ht}}{dt} = \frac{dI_M}{dt} = \frac{dH_M}{dt} = \frac{dR_M}{dt} = \frac{dS_F}{dt} = \frac{dE_F}{dt} = \frac{dI_F}{dt} = 0,$$

and solving the resulting algebraic system yields the malaria-free equilibrium point:

$$(S_M, E_{hm}, E_{ht}, I_M, H_M, R_M, S_F, E_F, I_F) = \left(\frac{\lambda_M}{\epsilon_M}, 0, 0, 0, 0, 0, \frac{\lambda_F}{\epsilon_F}, 0, 0\right).$$

At this equilibrium, the human and mosquito populations consist entirely of susceptible individuals, with no exposed or infected individuals present. This equilibrium plays a crucial role in stability analysis: if it is stable, malaria will eventually be eradicated from the population. The stability typically depends on the basic reproduction number R_0, which determines whether the disease can invade and persist.

3. Malaria-Present (Endemic) Equilibrium Point

The endemic equilibrium represents the steady state where malaria persists in both human and mosquito populations. Setting the derivatives in the system (2.3-2.11) to zero and solving algebraically yields the following expressions for each compartment. Equilibrium values are denoted

with an asterisk (e.g., $\mathbb{E}^*$).

$$\begin{aligned}
S_M^* &= \frac{\lambda_M(\epsilon_M+\varphi_M)(\mu_M+\epsilon_M+\rho_M)}{\alpha_M\beta_M\phi_M\varphi_M E_F^*/T_M^* + (\epsilon_M+\varphi_M)(\mu_M+\epsilon_M+\rho_M)(\epsilon_M+\gamma_M)} \\
E_{hm}^* &= \frac{\alpha_M\beta_M S_M^* I_F^*}{T_M^*(\epsilon_M+\varphi_M)}, \\
E_{ht}^* &= \frac{\gamma_M S_M^*}{\epsilon_M+\eta_M} \\
I_M^* &= \frac{\varphi_M E_{hm}^*}{\mu_M+\epsilon_M+\rho_M}, \\
H_M^* &= \frac{\rho_M I_M^*}{\mu_M+\epsilon_M+\delta_M} \\
R_M^* &= \frac{\eta_M E_{ht}^* + \delta_M H_M^*}{\epsilon_M+\omega_M} \\
S_F^* &= \frac{\lambda_F}{\epsilon_F + \frac{\alpha_M\beta_F I_M^*}{T_F} - \frac{\alpha_M\beta_M R_M^*}{T_F}} \\
E_F^* &= \frac{S_F^*\left(\frac{\alpha_M\beta_F I_M^*}{T_F} + \frac{\alpha_M\beta_M R_M^*}{T_F}\right)}{\phi_M+\epsilon_F} \\
I_F^* &= \frac{\phi_M E_F^*}{\epsilon_F}
\end{aligned} \tag{3.13}$$

3.1. Basic Reproduction Number

The basic reproduction number, R_0, quantifies the average number of secondary infections generated by a single infected mosquito or human in a completely susceptible population. To calculate R_0, we employ the next-generation matrix method as presented by Van den Driessche and Watmough [40]. This approach focuses on the infectious compartments and incorporates both transmission and transition processes within and between these classes. The next-generation matrix is defined as FV^{-1}, where the matrix F includes terms associated with new infections, and V consists of transition terms excluding new infections. The basic reproduction number R_0 is given by the spectral radius (dominant eigenvalue) of FV^{-1}, denoted by $\rho(FV^{-1})$. The matrices F and V are expressed as:

$$F = \begin{bmatrix} 0 & 0 & 0 & 0 & 0 & \alpha_M\beta_M \\ 0 & 0 & 0 & 0 & 0 & 0 \\ 0 & 0 & 0 & 0 & 0 & 0 \\ 0 & 0 & 0 & 0 & 0 & 0 \\ 0 & \alpha_M\beta_M & 0 & 0 & 0 & 0 \\ 0 & 0 & 0 & 0 & 0 & 0 \end{bmatrix}, \tag{3.14}$$

$$V = \begin{bmatrix} \epsilon_M + \varphi_M & 0 & 0 & 0 & 0 & 0 \\ -\varphi_M & \mu_M + \epsilon_M + \rho_M & 0 & 0 & 0 & 0 \\ 0 & -\rho_M & \mu_M + \epsilon_M + \delta_M & 0 & 0 & 0 \\ 0 & 0 & -\delta_M & \epsilon_M + \omega_M & 0 & 0 \\ 0 & 0 & 0 & 0 & \phi_M + \epsilon_F & 0 \\ 0 & 0 & 0 & 0 & -\phi_M & \epsilon_F \end{bmatrix}. \tag{3.15}$$

The product FV^{-1} is

$$FV^{-1} = \begin{bmatrix} 0 & 0 & 0 & 0 & 0 & \frac{\alpha_M \beta_M}{\epsilon_M + \varphi_M} \\ 0 & 0 & 0 & 0 & 0 & \frac{\varphi_M \alpha_M \beta_M}{(\epsilon_M + \varphi_M)(\mu_M + \epsilon_M + \rho_M)} \\ 0 & 0 & 0 & 0 & 0 & \frac{\rho_M \varphi_M \alpha_M \beta_M}{(\epsilon_M + \varphi_M)(\mu_M + \epsilon_M + \rho_M)(\mu_M + \epsilon_M + \delta_M)} \\ 0 & 0 & 0 & 0 & 0 & \frac{\delta_M \rho_M \varphi_M \alpha_M \beta_M}{(\epsilon_M + \varphi_M)(\mu_M + \epsilon_M + \rho_M)(\mu_M + \epsilon_M + \delta_M)(\epsilon_M + \omega_M)} \\ 0 & \frac{\alpha_M \beta_M}{\phi_M + \epsilon_F} & 0 & 0 & 0 & 0 \\ 0 & \frac{\phi_M \alpha_M \beta_M}{(\phi_M + \epsilon_F)\epsilon_F} & 0 & 0 & 0 & 0 \end{bmatrix}. \tag{3.16}$$

The dominant eigenvalue, which defines the basic reproduction number R_0, is

$$R_0 = \frac{\sqrt{\epsilon_F(\phi_F + \epsilon_F)(\epsilon_M + \varphi_M)(\mu_M + \epsilon_M + \rho_M)\phi_F \alpha_F \beta_F \varphi_M \alpha_M \beta_M}}{(\phi_F + \epsilon_F)\epsilon_F(\epsilon_M + \varphi_M)(\mu_M + \epsilon_M + \rho_M)}. \tag{3.17}$$

The behavior of R_0 with respect to different parameter values is illustrated in Figure 3. This analysis provides insight into how each parameter influences malaria transmission dynamics, which is essential for designing effective control strategies.

3.2. Global Stability of the Malaria-Free Equilibrium Point

Following the approach in [41], the system can be represented in a triangular form to analyze the global stability of an equilibrium point:

$$\begin{cases} \frac{dA_1}{dt} = X(A_1, A_2), \\ \frac{dA_2}{dt} = Y(A_1, A_2), \end{cases} \tag{3.18}$$

where

$$H(A_1, A_2) = 0.$$

At the malaria-free equilibrium point (MFEP), the uninfected population is denoted by $A_1 \in \mathbb{R}^2$, while the infected population is represented by $A_2 \in \mathbb{R}^7$. The criterion for global stability at the IFEP is given by

$$\frac{dA_1}{dt} = X(A_1, 0) = 0, \tag{3.19}$$

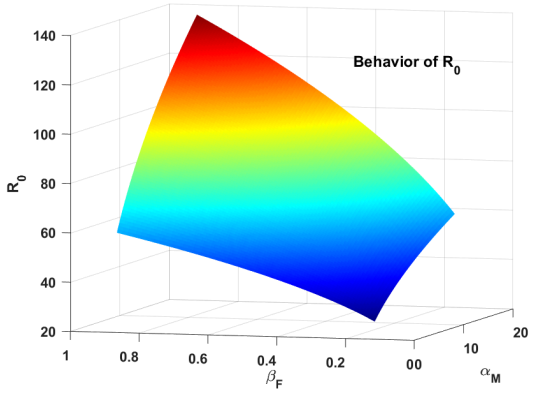

(a) *Behavior of* R_0 *between* α_M *and* β_F

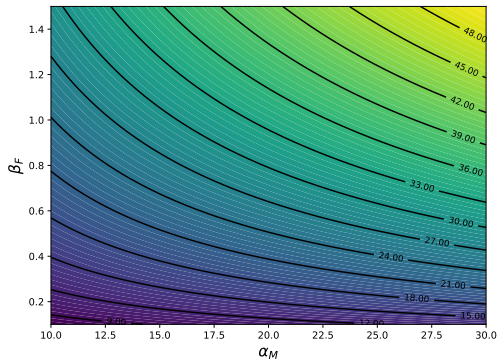

(b) *Effect of varying* α_M *and* β_M *on the reproduction number* R_0

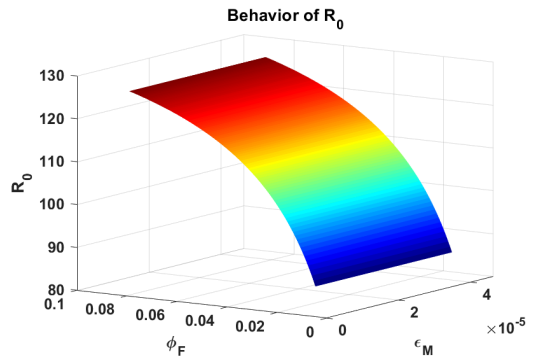

(c) *Behavior of* R_0 *between* ϕ_F *and* ϵ_M

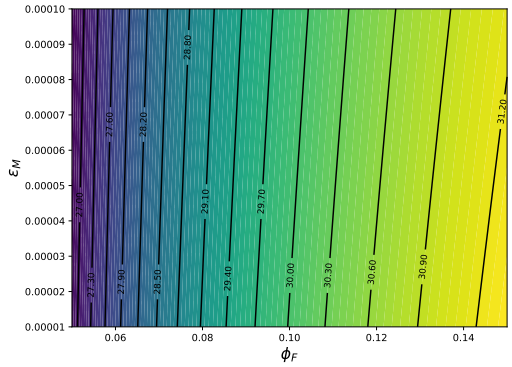

(d) *Effect of varying* ϕ_F *and* ϵ_M *on the reproduction number* R_0

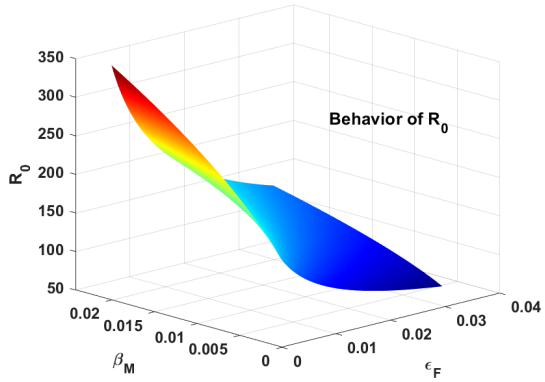

(e) *Behavior of* R_0 *between* ϵ_F *and* β_M

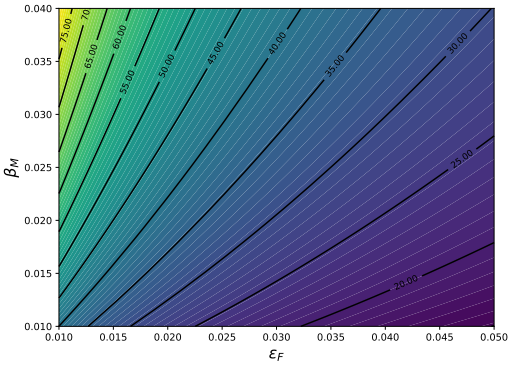

(f) *Effect of varying* β_M *and* ϵ_F *on the reproduction number* R_0

Figure 3: *Behavior of* R_0 *at sensitive parameters*

and

$$H(A_1, A_2) = P_1 N_{G^*} - \hat{H}(A_1, A_2). \tag{3.20}$$

Theorem 3. *The system of equations* (2.3)–(2.11) *is globally asymptotically stable at the malaria-free equilibrium point if* $R_0 < 1$.

Proof. To verify condition (3.19), consider the malaria-free equilibrium point

$$\mathbb{E}_0 = \left(K^0, 0\right) = (S_M, E_{hm}, E_{ht}, I_M, H_M, R_M, S_F, E_F, I_F) = \left(\frac{\lambda_M}{\epsilon_M}, 0, 0, 0, 0, 0, \frac{\lambda_F}{\epsilon_F}, 0, 0\right).$$

The subsystem for the uninfected classes reduces to

$$\frac{dA_1}{dt} = X(A_1, 0), \tag{3.21}$$

with

$$\begin{cases} \frac{dS_M^*}{dt} = \lambda_M - \epsilon_M S_M^*, \\ \frac{dS_F^*}{dt} = \lambda_F - \epsilon_F S_F^*. \end{cases} \tag{3.22}$$

Solving (3.22) yields the unique equilibrium

$$(S_M^*, E_{hm}, E_{ht}, I_M, H_M, R_M, S_F^*, E_F, I_F) = \left(\frac{\lambda_M}{\epsilon_M}, 0, 0, 0, 0, 0, \frac{\lambda_F}{\epsilon_F}, 0, 0\right),$$

which satisfies the global asymptotic stability condition for X^0. Next, to verify condition (3.20), define

$$F(A_1, A_2) = P_1 N_{A^*} - \hat{Y}(A_1, A_2),$$

where

$$\hat{Y}(A_1, A_2) \geq 0,$$

and

$$H(A_1, A_2) = \begin{bmatrix} \frac{\alpha_M \beta_M S_M I_F}{T_M} - \epsilon_M E_{hm} - \varphi_M E_{hm} \\ \gamma_M S_M - (\epsilon_M + \eta_M) E_{ht} \\ \varphi_M E_{hm} - (\mu_M + \epsilon_M + \rho_M) I_M \\ \rho_M I_M - (\mu_M + \epsilon_M + \delta_M) H_M \\ \delta_M H_M - \epsilon_M R_M - \omega_M R_M + \eta_M E_{ht} \\ \frac{\alpha_F \beta_F S_F I_M}{T_F} + \frac{\alpha_F \beta_F I_M R_M}{T_F} - \phi_F E_F - \epsilon_F E_F \\ \phi_F E_F - \epsilon_F I_F \end{bmatrix},$$

$$N_A^* = \begin{bmatrix} (-\epsilon_M - \varphi_M) E_{hm} + \frac{\alpha_M \beta_M S_M^* I_F}{T_M} \\ (-\epsilon_M - \eta_M) E_{ht} \\ \varphi_M E_{hm} + (-\mu_M - \epsilon_M - \rho_M) I_M \\ \rho_M I_M + (-\mu_M - \epsilon_M - \delta_M) H_M \\ \eta_M \omega + \delta_M H_M + (-\epsilon_M - \omega_M) R_M \\ \left(\frac{\alpha_F \beta_F S_F^*}{T_F} + \frac{\alpha_F \beta_F R_M}{T_F}\right) I_M + \frac{\alpha_F \beta_F I_M R_M}{T_F} + (-\phi_F - \epsilon_F) E_F \\ \phi_F E_F - \epsilon_F I_F \end{bmatrix},$$

and

$$\hat{Y}(A_1, A_2) = \begin{bmatrix} \frac{\beta_M c \alpha_M (S_M^* - S_M)}{T_M} \\ 0 \\ 0 \\ 0 \\ 0 \\ \frac{\beta_F \alpha_F I_M (S_F^* - S_F + R_M)}{T_F} \\ 0 \end{bmatrix} \geq 0.$$

Since $\hat{Y}(A_1, A_2) \geq 0$, conditions (3.19) and (3.20) hold. Therefore, the system is globally asymptotically stable at the malaria-free equilibrium point when $R_0 < 1$, which completes the proof of Theorem 3.

Table 1: *Descriptions of Model Parameters*

Parameter	Meaning
λ_M	Growth rate of the human population.
β_F	Transmission rate of malaria parasites from infected humans to susceptible mosquitoes.
β_M	Transmission rate of malaria parasites from infected mosquitoes to susceptible humans.
α_M	Rate at which mosquitoes bite humans.
ϵ_M	Natural mortality rate of humans.
ψ_M	Transition rate of humans from exposed to infected class.
ρ_M	Rate at which infected humans move to hospitalization.
μ_M	Malaria-induced mortality rate in humans.
δ_M	Rate of recovery from hospitalization to recovered class.
λ_F	Recruitment rate of the mosquito population.
ϵ_F	Natural death rate of mosquitoes.
ϕ_F	Rate at which mosquitoes progress from exposed to infectious stage.
η_M	Recovery rate of heterogeneous exposed humans.

4. Global Stability of the Malaria-Present Equilibrium Point

Theorem 4. *Consider the malaria transmission model defined by Equations (2.3-2.11). If the basic reproduction number $\mathcal{R}_0 > 1$, then the endemic equilibrium $\mathbb{E}^* = (S_M^*, E_{hm}^*, \ldots, I_F^*)$ is globally asymptotically stable in the interior of the feasible region $\Omega^T = \{(S_M, \ldots, I_F) \in \mathbb{R}_+^9\}$.*

Proof. We prove global stability using a Lyapunov function and LaSalle's Invariance Principle. Define the Lyapunov function [42]:

$$L = \sum_i \left(x_i - x_i^* - x_i^* \ln \frac{x_i}{x_i^*} \right), \tag{4.23}$$

where x_i represents the model compartments and x_i^* their endemic equilibrium values. The time derivative of L is:

$$\frac{dL}{dt} = \sum_i \left(1 - \frac{x_i^*}{x_i}\right) \frac{dx_i}{dt}. \tag{4.24}$$

Substituting the model equations and simplifying, we obtain:

$$\begin{aligned}
\left(1 - \frac{S_M^*}{S_M}\right) \frac{dS_M}{dt} &= \left(1 - \frac{S_M^*}{S_M}\right) \left[\lambda_M - \frac{\alpha_M \beta_M S_M I_F}{T_M} - \epsilon_M S_M + \omega_M R_M - \gamma_M S_M\right], \\
\left(1 - \frac{E_{hm}^*}{E_{hm}}\right) \frac{dE_{hm}}{dt} &= \left(1 - \frac{E_{hm}^*}{E_{hm}}\right) \left[\frac{\alpha_M \beta_M S_M I_F}{T_M} - (\epsilon_M + \varphi_M) E_{hm}\right], \\
\left(1 - \frac{I_M^*}{I_M}\right) \frac{dI_M}{dt} &= \left(1 - \frac{I_M^*}{I_M}\right) \left[\varphi_M E_{hm} - (\mu_M + \epsilon_M + \rho_M) I_M\right], \\
\left(1 - \frac{S_F^*}{S_F}\right) \frac{dS_F}{dt} &= \left(1 - \frac{S_F^*}{S_F}\right) \left[\lambda_F - \frac{\alpha_M \beta_F S_F I_M}{T_F} + \frac{\alpha_M \beta_M R_M S_F}{T_F} - \epsilon_F S_F\right], \\
\left(1 - \frac{E_F^*}{E_F}\right) \frac{dE_F}{dt} &= \left(1 - \frac{E_F^*}{E_F}\right) \left[\frac{\alpha_M \beta_F S_F I_M}{T_F} + \frac{\alpha_M \beta_M R_M S_F}{T_F} - (\phi_M + \epsilon_F) E_F\right].
\end{aligned} \tag{4.25}$$

Using equilibrium conditions and algebraic identities:

$$\begin{aligned}
\frac{dL}{dt} =& -\epsilon_M \frac{(S_M - S_M^*)^2}{S_M} - \epsilon_F \frac{(S_F - S_F^*)^2}{S_F} \\
&+ \frac{\alpha_M \beta_M S_M^* I_F^*}{T_M^*} \left[4 - \frac{S_M^*}{S_M} - \frac{E_{hm} S_M I_F^*}{E_{hm}^* S_M^* I_F} - \frac{E_{hm}^* I_F}{E_{hm} I_F^*} - \frac{S_M I_F}{S_M^* I_F^*}\right] \\
&+ \frac{\alpha_M \beta_F S_F^* I_M^*}{T_F^*} \left[3 - \frac{S_F^*}{S_F} - \frac{E_F S_F I_M^*}{E_F^* S_F^* I_M} - \frac{E_F^* I_M}{E_F I_M^*}\right] - \Omega^T,
\end{aligned}$$

where $\Omega^T > 0$ contains mortality/progression terms. By the Arithmetic Mean-Geometric Mean (AM-GM) inequality:

$$\begin{aligned}
4 - \frac{S_M^*}{S_M} - \frac{E_{hm} S_M I_F^*}{E_{hm}^* S_M^* I_F} - \frac{E_{hm}^* I_F}{E_{hm} I_F^*} - \frac{S_M I_F}{S_M^* I_F^*} \leq 0 \\
3 - \frac{S_F^*}{S_F} - \frac{E_F S_F I_M^*}{E_F^* S_F^* I_M} - \frac{E_F^* I_M}{E_F I_M^*} \leq 0
\end{aligned}$$

Equality holds iff:

$$\frac{S_M}{S_M^*} = \frac{E_{hm}}{E_{hm}^*} = \frac{I_F}{I_F^*} \quad \text{and} \quad \frac{S_F}{S_F^*} = \frac{E_F}{E_F^*} = \frac{I_M}{I_M^*},$$

Thus, $\frac{dL}{dt} \leq 0$ for all $(S_M, \ldots, I_F) \in \Gamma^\circ$, with equality only when:

$$S_M = S_M^*,\ E_{hm} = E_{hm}^*,\ I_F = I_F^*,\ S_F = S_F^*,\ E_F = E_F^*,\ I_M = I_M^*.$$

The largest invariant set where $\frac{dL}{dt} = 0$ is $\mathbb{E}^*$. By LaSalle's principle, all trajectories in Ω^T converge to $\mathbb{E}^*$ as $t \to \infty$. Thus, for $\mathcal{R}_0 > 1$, $\mathbb{E}^*$ is globally asymptotically stable in Ω^T.

4.1. Sensitivity Analysis

Understanding the parameters that influence the basic reproduction number R_0 is crucial for guiding effective malaria control strategies. Sensitivity analysis [43–45] plays a pivotal role in identifying key parameters that should be prioritized, especially when resources are limited. The normalized forward sensitivity index of a variable W, which depends on a parameter p, is defined as [46]:

$$\omega_p^W = \frac{\partial W}{\partial p} \times \frac{p}{W}. \tag{4.26}$$

According to this definition, a larger magnitude of the sensitivity index indicates a greater influence of the parameter p on the variable W. Applying this to the basic reproduction number R_0, the sensitivity index is given by:

$$\omega_p^{R_0} = \frac{\partial R_0}{\partial p} \times \frac{p}{R_0}. \tag{4.27}$$

The sensitivity indices of key parameters affecting R_0 are computed as follows:

$$\begin{aligned}
&\omega_{\phi_M}^{R_0} = \frac{\epsilon_F}{2\phi_M + 2\epsilon_F} > 0, \quad \omega_{\epsilon_F}^{R_0} = -\frac{\phi_M + 2\epsilon_F}{2\phi_M + 2\epsilon_F} < 0, \quad \omega_{\varphi_M}^{R_0} = \frac{\epsilon_M}{2\epsilon_M + 2\varphi_M} > 0, \\
&\omega_{\rho_M}^{R_0} = -\frac{\rho_M}{2\mu_M + 2\epsilon_M + 2\rho_M} < 0, \quad \omega_{\mu_M}^{R_0} = -\frac{\mu_M}{2\mu_M + 2\epsilon_M + 2\rho_M} < 0, \quad \omega_{\beta_M}^{R_0} = 1, \\
&\omega_{\epsilon_M}^{R_0} = -\frac{(\mu_M + \rho_M + 2\epsilon_M + \varphi_M)\epsilon_M}{2(\epsilon_M + \varphi_M)(\mu_M + \epsilon_M + \rho_M)}, \quad \omega_{\alpha_M}^{R_0} = 1.
\end{aligned} \tag{4.28}$$

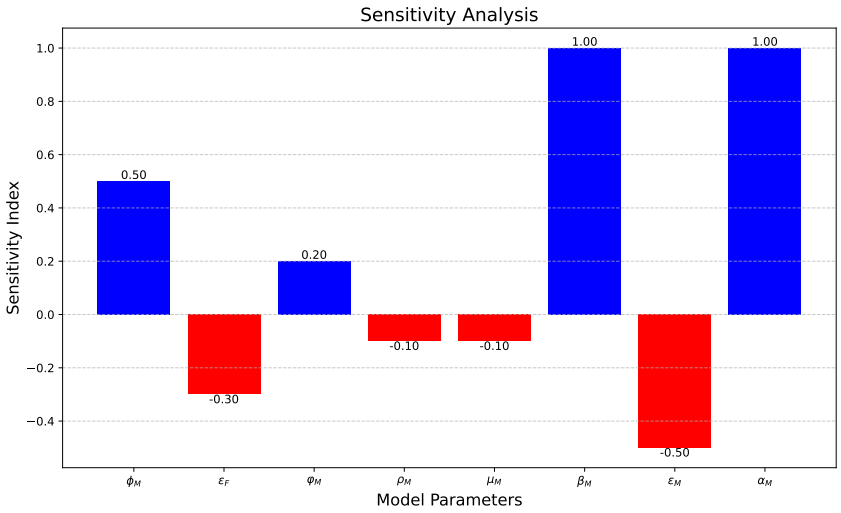

Figure 4: *Sensitivity Analysis of the Basic Reproduction Number* R_0.

Figure 4 illustrates the sensitivity indices of R_0 with respect to various parameters. This analysis highlights which parameters have the greatest impact on malaria transmission dynamics, thereby informing targeted intervention strategies.

5. Optimal Control

To control the transmission of malaria, we examine the effects of medicinal treatments and preventive measures through a set of time-dependent control variables m_1, m_2, and m_3, defined as follows:

(i) Provision of treated pesticide bed nets to the susceptible population, represented by m_1,

(ii) Treatment of the infected population, represented by m_2,

(iii) Insecticide spray application, represented by m_3.

The mathematical model incorporating these optimal controls m_1, m_2, and m_3 is described by the following non-autonomous system of nonlinear ordinary differential equations:

$$\frac{dS_M}{dt} = \lambda_M - \frac{m_1\alpha_M\beta_M S_M I_F}{T_M} - \epsilon_M S_M + \omega_M R_M - \gamma_M S_M, \tag{5.29}$$

$$\frac{dE_{hm}}{dt} = \frac{m_1\alpha_M\beta_M S_M I_F}{T_M} - \epsilon_M E_{hm} - \varphi_M E_{hm}, \tag{5.30}$$

$$\frac{dE_{ht}}{dt} = \gamma_M S_M - (\epsilon_M + \eta_M)E_{ht}, \tag{5.31}$$

$$\frac{dI_M}{dt} = \varphi_M E_{hm} - (\mu_M + \epsilon_M + m_2\rho_M)I_M, \tag{5.32}$$

$$\frac{dH_M}{dt} = m_2\rho_M I_M - (\mu_M + \epsilon_M + \delta_M)H_M, \tag{5.33}$$

$$\frac{dR_M}{dt} = \eta_M E_{ht} + \delta_M H_M - \epsilon_M R_M - \omega_M R_M, \tag{5.34}$$

$$\frac{dS_F}{dt} = \lambda_F - m_3\left(\frac{\alpha_M\beta_M S_F I_M}{T_F} + \frac{\alpha_M\beta_M R_M S_F}{T_F}\right) - (m_1 + m_3)\epsilon_F S_F, \tag{5.35}$$

$$\frac{dE_F}{dt} = m_3\left(\frac{\alpha_M\beta_M S_F I_M}{T_F} + \frac{\alpha_M\beta_M R_M S_F}{T_F}\right) - \phi_M E_F - (m_1 + m_3)\epsilon_F E_F, \tag{5.36}$$

$$\frac{dI_F}{dt} = \phi_M E_F - (m_1 + m_3)\epsilon_F I_F. \tag{5.37}$$

Our goal is to find the optimal control functions (m_1^*, m_2^*, m_3^*) that minimize the objective functional

$$\begin{aligned} J(m_1, m_2, m_3) = \min_{m_1,m_2,m_3} \int_0^T \Big[& P_1 E_{hm} + P_2 E_{ht} + P_3 I_M + P_4 E_F + P_5 I_F \\ & + L_1 m_1(t)^2 + L_2 m_2(t)^2 + L_3 m_3(t)^2 \Big] dt, \end{aligned} \tag{5.38}$$

where T is the final time, P_1, P_2, P_3, P_4, P_5 are weight parameters representing the relative costs associated with exposed and infected human and mosquito populations, and L_1, L_2, L_3 are the weight costs associated with implementing the control measures.

Following the approach in [47, 48], the control costs are modeled by quadratic functions to ensure convexity and satisfy optimality conditions.

The optimal controls satisfy

$$J(m_1^*, m_2^*, m_3^*) = \min_{(m_1,m_2,m_3)\in\mathbb{U}} J(m_1, m_2, m_3),$$

where the admissible control set is defined as

$$\mathbb{U} = \{(m_1, m_2, m_3) \mid m_i(t) \text{ is Lebesgue measurable on } [0, T], \quad 0 \le m_i(t) \le 1, \quad i = 1, 2, 3\}.$$

5.1. Hamiltonian and Its Optimality Equation

Using Pontryangin's Maximum Principle [PMP] [49], one may ascertain what conditions an optimal control must meet. His principle converts equations (5.29 - 5.37) and (5.38) into a problem of minimization of the point-wise hamiltonian ($\mathbb{H}$) with regard to $m_1(t), m_2(t)$, and $m_3(t)$.

$$\begin{aligned}
\mathbb{H} &= P_1 E_{hm} + P_2 E_{ht} + P_3 I_M + P_4 E_F + P_5 I_F + L_1 (m_1(t))^2 + L_2 (m_2(t))^2 + L_3 (m_3(t))^2 \\
&+ \Xi_1[\lambda_M - \frac{m_1 \alpha_M \beta_M S_M I_F}{T_M} - \epsilon_M S_M + \omega_M R_M - \gamma_M S_M] \\
&+ \Xi_2[\frac{m_1 \alpha_M \beta_M S_M I_F}{T_M} - \epsilon_M E_{hm} - \varphi_M E_{hm}] \\
&+ \Xi_3[\gamma_M S_M - (\epsilon_M + \eta_M) E_{ht}] \\
&+ \Xi_4[\varphi_M E_{hm} - (\mu_M + \epsilon_M + m_2 \rho_M) I_M] \\
&+ \Xi_5[m_2 \rho_M I_M - (\mu_M + \epsilon_M + \delta_M) H_M] \\
&+ \Xi_6[\eta_M E_{ht} + \delta_M H_M - \epsilon_M R_M - \omega_M R_M] \\
&+ \Xi_7[\lambda_F - m_3 \left(\frac{\alpha_M \beta_M S_F I_M}{T_F} + \frac{\alpha_M \beta_M R_M S_F}{T_F}\right) - (m_1 + m_3)\epsilon_F S_F] \\
&+ \Xi_8[m_3 \left(\frac{\alpha_M \beta_M S_F I_M}{T_F} + \frac{\alpha_M \beta_M R_M S_F}{T_F}\right) - \phi_M E_F - (m_1 + m_3)\epsilon_F E_F] \\
&+ \Xi_9[-(m_1 + m_3)\epsilon_F I_F + \phi_M E_F].
\end{aligned} \tag{5.39}$$

Where (Ξ_i), $i = 1, 2, \ldots, 9.$ are adjoint variables associate with $S_M, E_{ht}, E_{hm}, I_M, H_M, R_M, S_F, E_F$ and, I_F.

Theorem 5. *For the optimal control (a_2^*, a_2^*, a_3^*) and, corresponding state solution,*

$$S_M, E_{ht}, E_{hm}, I_M, H_M, R_M, S_F, E_F, I_F$$

that minimize J over $\mathbb{U}$ of the corresponding system of equations (2.3 - 2.11) having the adjoint variable $\Xi_1, \ldots, \Xi_8$, such that,

$$\begin{cases} \frac{d\Xi_1}{dt} &= (\Xi_1-\Xi_2)\frac{m_1\alpha_M\,\beta_M\,I_F}{T_M}+\epsilon_M\Xi_1-(\Xi_3-\Xi_1)\,\gamma_M,\\ \frac{d\Xi_2}{dt} &= (\Xi_4-\Xi_2)\varphi_M+\epsilon_M\Xi_2-P_1,\\ \frac{d\Xi_3}{dt} &= (\Xi_6-\Xi_3)\eta_M+\epsilon_M\Xi_3-P_2,\\ \frac{d\Xi_4}{dt} &= (\Xi_8-\Xi_7)m_3\left(\frac{\alpha_M\,\beta_M\,S_F}{T_F}\right)+(\Xi_3-\Xi_4)m_2\rho_M+(\mu_M+\epsilon_M)\Xi_3-P_3,\\ \frac{d\Xi_5}{dt} &= \Xi_5-\Xi_4)\delta_M+(\mu_M+\epsilon_M)\Xi_4,\\ \frac{d\Xi_6}{dt} &= (\Xi_6-\Xi_5)\frac{m_1\alpha_M\,\beta_M\,S_F}{T_M}+(\Xi_1-\Xi_6)\,\eta_M+\Xi_6\epsilon_M,\\ \frac{d\Xi_7}{dt} &= (\Xi_7-\Xi_8)m_3\left(\frac{\alpha_M\,\beta_M\,I_M}{T_F}+\frac{\alpha_M\,\beta_M\,R_M}{T_F}\right)+(m_1+m_3)\epsilon_F\Xi_7\\ \frac{d\Xi_8}{dt} &= (\Xi_8-\Xi_9)\phi_M+(m_1+m_3)\epsilon_F\Xi_8-P_4,\\ \frac{d\Xi_9}{dt} &= (\Xi_7-\Xi_8)\frac{m_1\alpha_M\,\beta_M\,S_F}{T_M}+(m_1+m_3)\epsilon_F\Xi_9-P_5. \end{cases} \tag{5.40}$$

With conditions, $\Xi_i(T)=0$*, for* $i=1,2,3,\ldots,9$.

furthermore, the control set obtain (m_1^*,m_2^*,m_3^*) *component of,*

$$\begin{aligned} m_1^* &= max\{0,min(1,\Omega_1)\},\\ m_2^* &= max\{0,min(1,\Omega_2)\},\\ m_3^* &= max\{0,min(1,\Omega_3)\}. \end{aligned} \tag{5.41}$$

Where,

$$\begin{aligned} \Omega_1 &= \frac{(\Xi_2-\Xi_1)\frac{\alpha_M\,\beta_M\,S_M\,I_F}{T_M}-(\Xi_7+\Xi_6+\Xi_8)\epsilon_F S_F}{2L_1},\\ \Omega_2 &= \frac{(\Xi_5-\Xi_4)\rho_M}{2L_2},\\ \Omega_3 &= \frac{(\Xi_8-\Xi_7)\left(\frac{\alpha_M\,\beta_M\,S_F\,I_M}{T_F}+\frac{\alpha_M\,\beta_M\,R_M\,S_F}{T_F}\right)-(\Xi_7+\Xi_6+\Xi_8)\epsilon_F S_F}{2Y_3}. \end{aligned} \tag{5.42}$$

Proof. Pontryagin's Maximal Principle yields the standard conclusions of the adjoint equation and transversality criteria [50].

The adjoint system is written as a result of differentiation of the Hamiltonian concerning the various states $S_M, E_{hm}, E_{ht}, I_M, H_M, R_M, S_F, E_F$ and I_F.

$$\frac{d\Xi_1}{dt}=-\frac{\mathrm{d}\mathbb{H}}{\mathrm{d}S_M}=(\Xi_1-\Xi_2)\frac{m_1\alpha_M\beta_M I_F}{T_M}+\epsilon_M\Xi_1, \tag{5.43}$$

$$\frac{d\Xi_2}{dt}=-\frac{\mathrm{d}\mathbb{H}}{\mathrm{d}E_{hm}}=(\Xi_3-\Xi_2)\varphi_M S+\epsilon_M\Xi_2-P_1, \tag{5.44}$$

$$\frac{d\Xi_3}{dt}=-\frac{\mathrm{d}\mathbb{H}}{\mathrm{d}E_{ht}}=(\Xi_6-\Xi_3)\eta_M+\epsilon_M\Xi_3-P_2, \tag{5.45}$$

$$\frac{d\Xi_4}{dt}=-(\Xi_8-\Xi_7)m_3\left(\frac{\alpha_M\beta_M S_F}{T_F}\right)+(\Xi_3-\Xi_4)m_2\rho_M+(\mu_M+\epsilon_M)\Xi_3-P_3, \tag{5.46}$$

$$\frac{d\Xi_5}{dt} = -(\Xi_5 - \Xi_4)\delta_M + (\mu_M + \epsilon_M)\Xi_4, \tag{5.47}$$

$$\frac{d\Xi_6}{dt} = -(\Xi_6 - \Xi_5)\frac{m_1\alpha_M\beta_M S_F}{T_M} + (\Xi_1 - \Xi_6)\eta_M + \Xi_6\epsilon_M, \tag{5.48}$$

$$\frac{d\Xi_7}{dt} = -(\Xi_7 - \Xi_8)m_3\left(\frac{\alpha_M\beta_M I_M}{T_F} + \frac{\alpha_M\beta_M R_M}{T_F}\right) + (m_1 + m_3)\epsilon_F\Xi_7, \tag{5.49}$$

$$\frac{d\Xi_8}{dt} = -(\Xi_8 - \Xi_9)\phi_M + (m_1 + m_3)\epsilon_F\Xi_8 - P_4, \tag{5.50}$$

$$\frac{d\Xi_9}{dt} = -(\Xi_7 - \Xi_8)\frac{m_1\alpha_M\beta_M S_F}{T_M} + (m_1 + m_3)\epsilon_F\Xi_9 - P_5, \tag{5.51}$$

With conditions, $\Xi_i(T) = 0$, for $i = 1, 2, 3, \ldots, 8$.
The optimal controls (m_1^*, m_2^*, m_3^*) are characterised by adopting the strategy used by Pontryagin [49], and the optimality equations are constructed based on the following conditions,
$\frac{\partial\mathbb{H}}{\partial m_i}$, for $i = 1, 2, 3, \ldots, 8$. which gives,

$$\begin{aligned}
\frac{\partial\mathbb{H}}{\partial m_1} &= \frac{(\Xi_2 - \Xi_1)\frac{\alpha_M\,\beta_M\,S_M\,I_F}{T_M} - (\Xi_7 + \Xi_6 + \Xi_8)\epsilon_F S_F}{2L_1},\\
\frac{\partial\mathbb{H}}{\partial m_2} &= \frac{(\Xi_4 - \Xi_3)\rho_M}{2L_2},\\
\frac{\partial\mathbb{H}}{\partial m_3} &= \frac{(\Xi_7 - \Xi_6)\left(\frac{\alpha_M\,\beta_M\,S_F\,I_M}{T_F} + \frac{\alpha_M\,\beta_M\,R_M\,S_F}{T_F}\right) - (\Xi_7 + \Xi_6 + \Xi_8)\epsilon_F S_F}{2L_3},
\end{aligned} \tag{5.52}$$

setting $\frac{\partial\mathbb{H}}{\partial m_i} = 0$,
for m_i^*, the results are,

$$\begin{aligned}
m_1^* &= \frac{(\Xi_2 - \Xi_1)\frac{\alpha_M\,\beta_M\,S_M\,I_F}{T_M} - (\Xi_7 + \Xi_6 + \Xi_8)\epsilon_F S_F}{2L_1},\\
m_2^* &= \frac{(\Xi_4 - \Xi_3)\rho_M}{2L_2},\\
m_3^* &= \frac{(\Xi_7 - \Xi_6)\left(\frac{\alpha_M\,\beta_M\,S_F\,I_M}{T_F} + \frac{\alpha_M\,\beta_M\,R_M\,S_F}{T_F}\right) - (\Xi_7 + \Xi_6 + \Xi_8)\epsilon_F S_F}{2L_3},
\end{aligned} \tag{5.53}$$

The boundaries on the controls will be written using common control parameters. As a result,

$$m_1^* = \begin{cases} \Omega_1, & \text{if } 0 < \Omega_1 < 1;\\ 0, & \text{if } \Omega_1 \le 0;\\ 1, & \text{if } \Omega_1 \ge 1. \end{cases}, \tag{5.54}$$

$$m_2^* = \begin{cases} \Omega_2, & \text{if } 0 < \Omega_2 < 1;\\ 0, & \text{if } \Omega_2 \le 0;\\ 1, & \text{if } \Omega_2 \ge 1. \end{cases}, \tag{5.55}$$

and,

$$m_3^* = \begin{cases} \Omega_3, & if\ \ 0 < \Omega_3 < 1; \\ 0, & if\ \ \Omega_3 \leq 0; \\ 1, & if\ \ \Omega_3 \geq 1. \end{cases} . \tag{5.56}$$

In concise notation,

$$\begin{aligned} m_1^* &= max\{0, min(1, \Omega_1)\}, \\ m_2^* &= max\{0, min(1, \Omega_2)\}, \\ m_3^* &= max\{0, min(1, \Omega_3)\}. \end{aligned} \tag{5.57}$$

By using the values of Ω_1, Ω_2, and Ω_3

$$m_1^* = \begin{cases} \frac{(\Xi_2 - \Xi_1)\frac{\alpha_M \beta_M S_M I_F}{T_M} - (\Xi_7 + \Xi_6 + \Xi_8)\epsilon_F S_F}{2L_1}, & if\ \ 0 < \frac{(\Xi_2 - \Xi_1)\frac{\alpha_M \beta_M S_M I_F}{T_M} - (\Xi_7 + \Xi_6 + \Xi_8)\epsilon_F S_F}{2L_1} < 1; \\ 0, & if\ \ \frac{(\Xi_2 - \Xi_1)\frac{\alpha_M \beta_M S_M I_F}{T_M} - (\Xi_7 + \Xi_6 + \Xi_8)\epsilon_F S_F}{2L_1} \leq 0; \\ 1, & if\ \ \frac{(\Xi_2 - \Xi_1)\frac{\alpha_M \beta_M S_M I_F}{T_M} - (\Xi_7 + \Xi_6 + \Xi_8)\epsilon_F S_F}{2L_1} \geq 1. \end{cases} , \tag{5.58}$$

$$m_2^* = \begin{cases} \frac{(\Xi_4 - \Xi_3)\rho_M}{2L_2}, & if\ \ 0 < \frac{(\Xi_4 - \Xi_3)\rho_M}{2L_2} < 1; \\ 0, & if\ \ \frac{(\Xi_4 - \Xi_3)\rho_M}{2L_2} \leq 0; \\ 1, & if\ \ \frac{(\Xi_4 - \Xi_3)\rho_M}{2L_2} \geq 1. \end{cases} , \tag{5.59}$$

and,

$$m_3^* = \begin{cases} \frac{(\Xi_7 - \Xi_6)\left(\frac{\alpha_M \beta_M S_F I_M}{T_F} + \frac{\alpha_M \beta_M R_M S_F}{T_F}\right) - (\Xi_7 + \Xi_6 + \Xi_8)\epsilon_F S_F}{2L_3}, & if\ \ 0 < \Omega_3 < 1; \\ 0, & if\ \ \Omega_3 \leq 0; \\ 1, & if\ \ \Omega_3 \geq 1. \end{cases} . \tag{5.60}$$

Briefly expressed,

$$\begin{aligned} m_1^* &= max\{0, min\left(1, \frac{(\Xi_2 - \Xi_1)\frac{\alpha_M \beta_M S_M I_F}{T_M} - (\Xi_7 + \Xi_6 + \Xi_8)\epsilon_F S_F}{2L_1}\right)\}, \\ m_2^* &= max\{0, min\left(1, \frac{(\Xi_4 - \Xi_3)\rho_M}{2L_2}\right)\}, \\ m_3^* &= max\{0, min\left(1, \frac{(\Xi_7 - \Xi_6)\left(\frac{\alpha_M \beta_M S_F I_M}{T_F} + \frac{\alpha_M \beta_M R_M S_F}{T_F}\right) - (\Xi_7 + \Xi_6 + \Xi_8)\epsilon_F S_F}{2L_3}\right)\}. \end{aligned} \tag{5.61}$$

By including the described control set, initial, and transversal conditions, the optimality system is

generated from the adjoint variable system and the optimal control system.

$$
\begin{aligned}
\frac{d\Xi_1}{dt} &= -\frac{\mathrm{d}\mathbb{H}}{\mathrm{d}S_M} = (\Xi_1 - \Xi_2)\frac{m_1\alpha_M\,\beta_M\,I_F}{T_M} + \epsilon_M\Xi_1,\\
\frac{d\Xi_2}{dt} &= -\frac{\mathrm{d}\mathbb{H}}{\mathrm{d}E_M} = (\Xi_3 - \Xi_2)\varphi_M S + \epsilon_M\Xi_2 - P_1,\\
\frac{d\Xi_3}{dt} &= -\frac{\mathrm{d}\mathbb{H}}{\mathrm{d}I_M} = (\Xi_7 - \Xi_6)m_3\left(\frac{\alpha_M\,\beta_M\,S_F}{T_F}\right) + (\Xi_3 - \Xi_4)m_2\rho_M + (\mu_M + \epsilon_M)\Xi_3 - P_2,\\
\frac{d\Xi_4}{dt} &= -\frac{\mathrm{d}\mathbb{H}}{\mathrm{d}H_M} = (\Xi_6 - \Xi_5)\delta_M + (\mu_M + \epsilon_M)\Xi_4,\\
\frac{d\Xi_5}{dt} &= -\frac{\mathrm{d}\mathbb{H}}{\mathrm{d}R_M} = (\Xi_6 - \Xi_7)\frac{m_1\alpha_M\,\beta_M\,S_F}{T_M} + \Xi_5\epsilon_M,\\
\frac{d\Xi_6}{dt} &= -\frac{\mathrm{d}\mathbb{H}}{\mathrm{d}S_F} = (\Xi_6 - \Xi_7)m_3\left(\frac{\alpha_M\,\beta_M\,I_M}{T_F} + \frac{\alpha_M\,\beta_M\,R_M}{T_F}\right) + (m_1 + m_3)\epsilon_F\Xi_6,\\
\frac{d\Xi_7}{dt} &= -\frac{\mathrm{d}\mathbb{H}}{\mathrm{d}E_F} = (\Xi_7 - \Xi_8)\phi_M + (m_1 + m_3)\epsilon_F\Xi_7 - P_3,\\
\frac{d\Xi_8}{dt} &= -\frac{\mathrm{d}\mathbb{H}}{\mathrm{d}I_F} = (\Xi_6 - \Xi_7)\frac{m_1\alpha_M\,\beta_M\,S_F}{T_M} + (m_1 + m_3)\epsilon_F\Xi_8 - P_4,\\
m_1^* &= \frac{(\Xi_2 - \Xi_1)\frac{\alpha_M\,\beta_M\,S_M\,I_F}{T_M} - (\Xi_7 + \Xi_6 + \Xi_8)\epsilon_F S_F}{2L_1},\\
m_2^* &= \frac{(\Xi_4 - \Xi_3)\rho_M}{2L_2},\\
m_3^* &= \frac{(\Xi_7 - \Xi_6)\left(\frac{\alpha_M\,\beta_M\,S_F\,I_M}{T_F} + \frac{\alpha_M\,\beta_M\,R_M\,S_F}{T_F}\right) - (\Xi_7 + \Xi_6 + \Xi_8)\epsilon_F S_F}{2L_3},\\
\Xi_i(T) &= 0. \quad i = 1, 2, 3, \ldots, 8.
\end{aligned}
\tag{5.62}
$$

With the initial conditions,
$S_M(0) = S_{M0},\ E_{mh}(0) = E_{mh0},\ E_{ht}(0) = E_{ht0},\ I_M(0) = I_{M0},\ H_M(0) = H_{M0},\ R(0) = R_{M0},\ S_F(0) = S_{F0},\ E_F(0) = E_{F0},\ I_F(0) = I_{F0}$.

6. Numerical Simulation

In this section, we will explore how different control strategies can influence the control of malaria and aim to identify the cost approach by employing numerical optimization techniques. The optimization process involves solving a set of eight nonlinear Differential Equations. To carry out this optimization we adopt a method. Initially, we make estimations for the control parameters shown in Table 2. Then simulate the system over time using a fourth-order Runge Kutta numerical integration method results shown in Figure 5.

6.1. Numerical Method

Here, we solve the optimality system from the previous sections using the Runge-Kutta fourth-order approach, which was developed in [51]. The following is a summary of this approach:

(i) Select a random number for m^* over $[0, T]$; in general, $(m^* = 0)$.

(ii) Utilizing the beginning conditions $x(t_0) = x_0$ and the previously mentioned value of m^*, solve the state system explicitly,

(iii) The adjoint system $\Xi(t)$ can be solved implicitly by taking into account the transversality criteria $\Xi(T)$ and the expressions of m^* and x^* that were previously estimated,

(iv) Replace $x(t)$ and $\Xi(t)$ with their respective expressions to update the expression of m^*,

(v) Check for convergence. If the values of the variables in the current iteration and previous iterations are comparable enough, return the real values as solutions. Otherwise, return to Step 2.

For the state and adjoint equations, we employ the following notations:

$$\begin{aligned}
\frac{dS_M}{dt} &= k_1\left(x(t), m(t)\right)\\
\frac{dE_{hm}}{dt} &= k_2\left(x(t), m(t)\right)\\
\frac{dE_{ht}}{dt} &= k_3\left(x(t), m(t)\right)\\
\frac{dI_M}{dt} &= k_4\left(x(t), m(t)\right)\\
\frac{dH_M}{dt} &= k_5\left(x(t), m(t)\right)\\
\frac{dR_M}{dt} &= k_6\left(x(t), m(t)\right)\\
\frac{dS_F}{dt} &= k_7\left(x(t), m(t)\right)\\
\frac{dE_F}{dt} &= k_8\left(x(t), m(t)\right)\\
\frac{dI_F}{dt} &= k_9\left(x(t), m(t)\right)
\end{aligned} \tag{6.63}$$

and

$$\begin{aligned}
\Xi_1'(t) &= h_1\left(x(t), \Xi(t), m(t)\right)\\
\Xi_2'(t) &= h_2\left(x(t), \Xi(t), m(t)\right)\\
\Xi_3'(t) &= h_3\left(x(t), \Xi(t), m(t)\right)\\
\Xi_4'(t) &= h_4\left(x(t), \Xi(t), m(t)\right)\\
\Xi_5'(t) &= h_5\left(x(t), \Xi(t), m(t)\right)\\
\Xi_6'(t) &= h_6\left(x(t), \Xi(t), m(t)\right)\\
\Xi_7'(t) &= h_7\left(x(t), \Xi(t), m(t)\right)\\
\Xi_8'(t) &= h_8\left(x(t), \Xi(t), m(t)\right)\\
\Xi_9'(t) &= h_9\left(x(t), \Xi(t), m(t)\right)
\end{aligned} \tag{6.64}$$

The approximation of each state variable $x_i, i = 1, 2, ..., 9$ given a step size h is given by:

$$x_n^{i+1} = x_n^i + \frac{h}{6}\left(\mathbb{K}_{i1} + 2\mathbb{K}_{i2} + 2\mathbb{K}_{i3} + \mathbb{K}_{i4}\right), \tag{6.65}$$

where

$$\begin{aligned} \mathbb{K}_{i1} &= \mathbb{K}_i(x), \\ \mathbb{K}_{i2} &= f_i\left(x + \frac{h}{2}\mathbb{K}_{i1}\right), \\ \mathbb{K}_{i3} &= f_i\left(x + \frac{h}{2}\mathbb{K}_{i2}\right), \\ \mathbb{K}_{i4} &= f_i\left(x + h\mathbb{K}_{i3}\right). \end{aligned} \tag{6.66}$$

The approximation for the adjoint vector is of the following form and is provided backward in time:

$$\Xi_j^{n-1} = \Xi_j^n - h\left(\frac{1}{6}\left(\mathbb{K}_1^j + 2\mathbb{K}_2^j + 2\mathbb{K}_3^j + \mathbb{K}_4^j\right)\right),$$

where

$$\begin{aligned} \mathbb{K}_1^j &= g_j(x), \\ \mathbb{K}_2^j &= g_j\left(x + \frac{h}{2}\mathbb{K}_1^j\right), \\ \mathbb{K}_3^j &= g_j\left(x + \frac{h}{2}\mathbb{K}_2^j\right), \\ \mathbb{K}_4^j &= g_j\left(x + h\mathbb{K}_3^j\right). \end{aligned}$$

Following these procedures, the controls' values $m_i^*, i = 1, 2, 3$ are updated by their corresponding equations, Eqs (5.54-5.56).

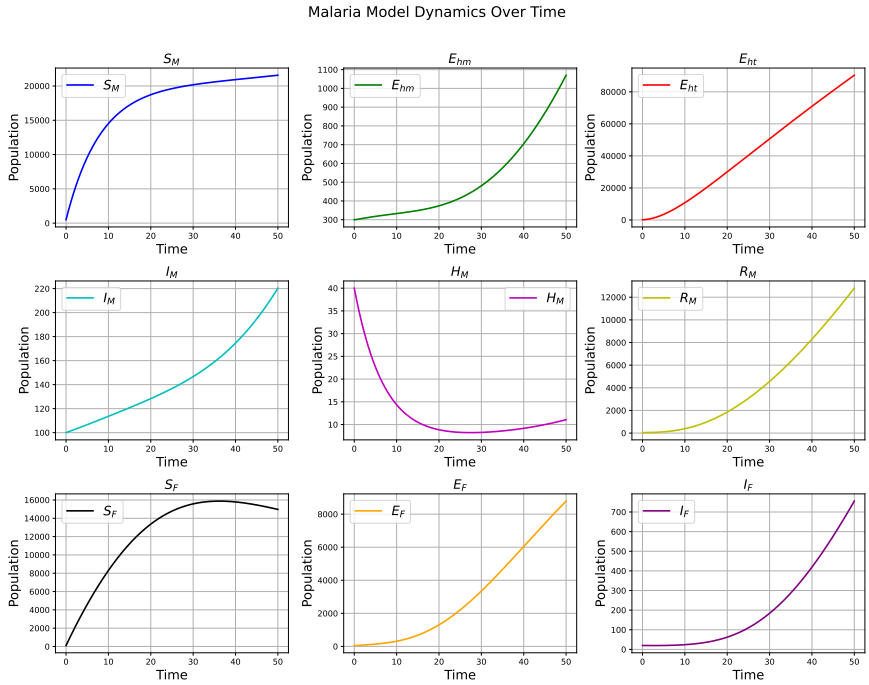

Figure 5: *Malaria Model Dynamics*

6.2. Phase Plot

Figure 6 illustrates the relationship between the number of infected mosquitoes and the likelihood of malaria transmission to humans. As the infected mosquito population increases, the risk of malaria transmission rises because infected mosquitoes are the primary vectors that bite humans and transmit the parasite. Consequently, a higher number of infected mosquitoes leads to more human infections. Similarly, an increase in susceptible mosquitoes results in a larger pool of mosquitoes available to bite susceptible humans, which can maintain or elevate the susceptible human population and potentially facilitate future infections if those mosquitoes become infected. Thus, the dynamics of mosquito infection directly influence human infection levels, while the abundance of susceptible mosquitoes affects the susceptibility of the human population to malaria transmission.

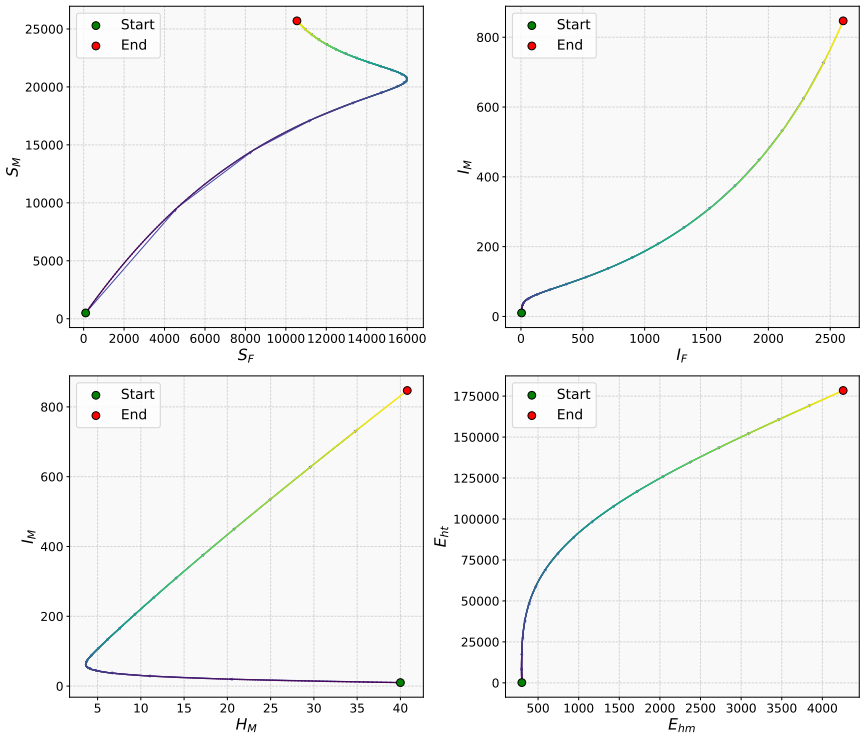

Figure 6: *Phase plane plots showing the interaction between susceptible and infected mosquito populations and their impact on malaria transmission.*

6.3. Control Strategies

6.3.1. Optimal Medication Treatment, Bed-nets & Insecticide Spray

To maximize the objective function $J(m_1, m_2, m_3)$, we implement controls on treated bed-nets (m_1), medication (m_2), and insecticide spray (m_3). Figure 7 demonstrates a significant reduction in the number of infected humans when these combined strategies are applied, especially after ten days. Additionally, the figure shows a decrease in the susceptible, exposed, and infected mosquito populations due to these interventions.

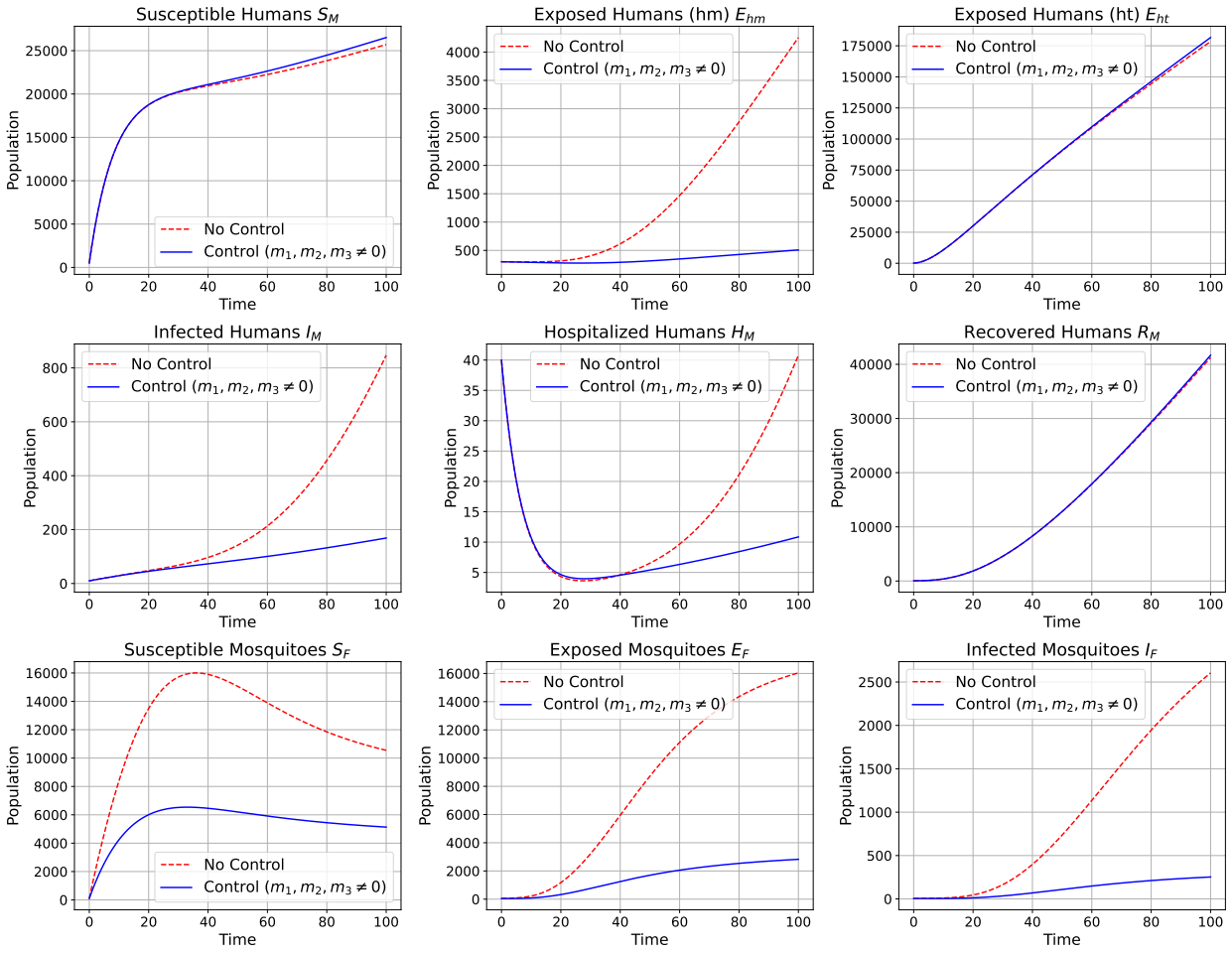

Figure 7: *Effect of combined optimal medication treatment, bed-nets, and insecticide spray on malaria dynamics.*

6.3.2. Medication & Insecticide Spray

This strategy employs medication (m_2) and insecticide spray (m_3) controls, with no bed-net intervention ($m_1 = 0$). Figure 8 shows a substantial decrease in infected humans after applying these controls, with effectiveness increasing after ten days. It also illustrates reductions in susceptible, exposed, and infected mosquito populations.

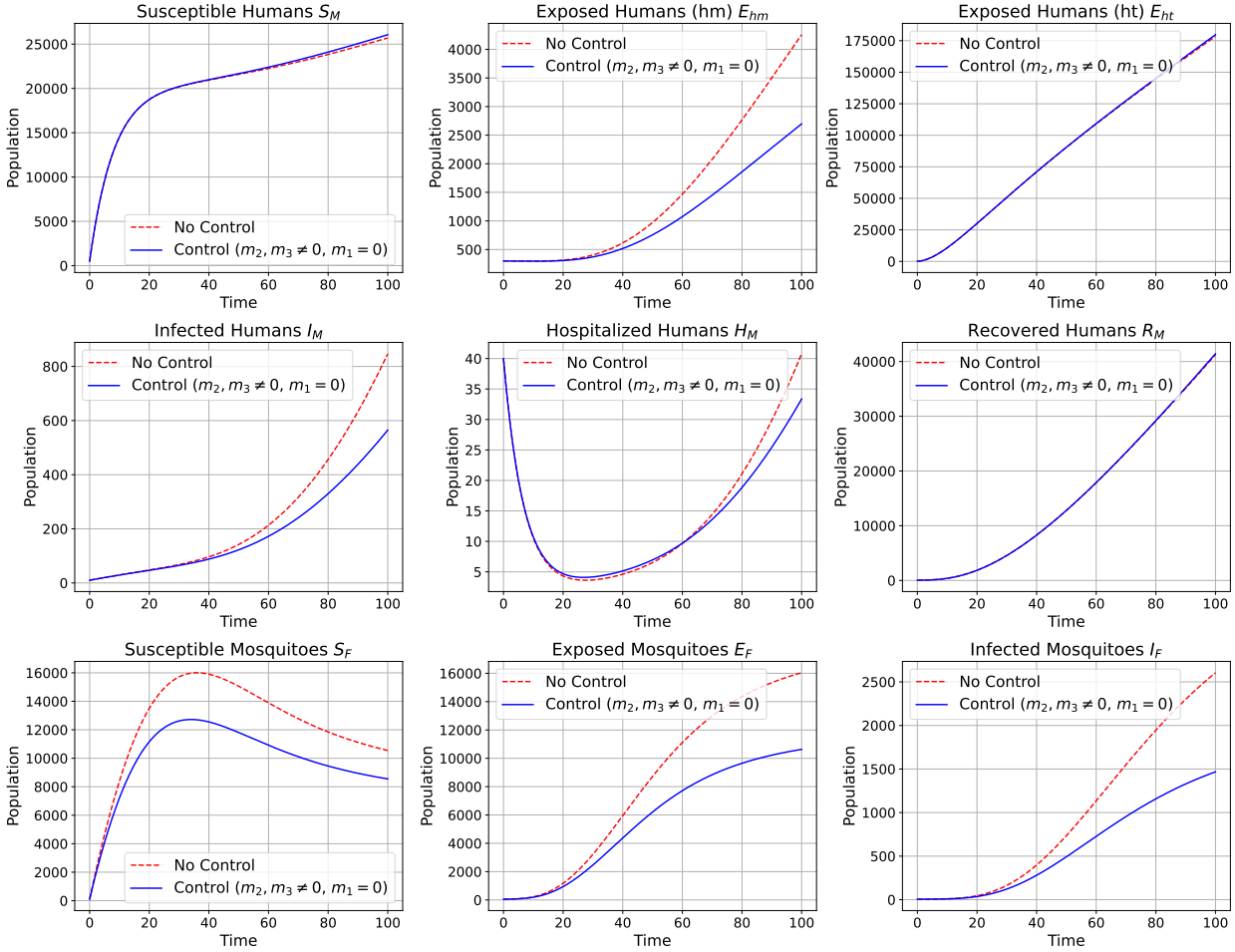

Figure 8: *Impact of medication and insecticide spray without bed-nets on malaria transmission.*

6.3.3. Optimal Bed-nets & Insecticide Spray

Here, controls on bed-nets (m_1) and insecticide spray (m_3) are applied, with no medication ($m_2 = 0$). Figure 9 shows that this combination significantly reduces the number of infected humans, especially after ten days. The figure also indicates decreases in susceptible, exposed, and infected mosquito populations.

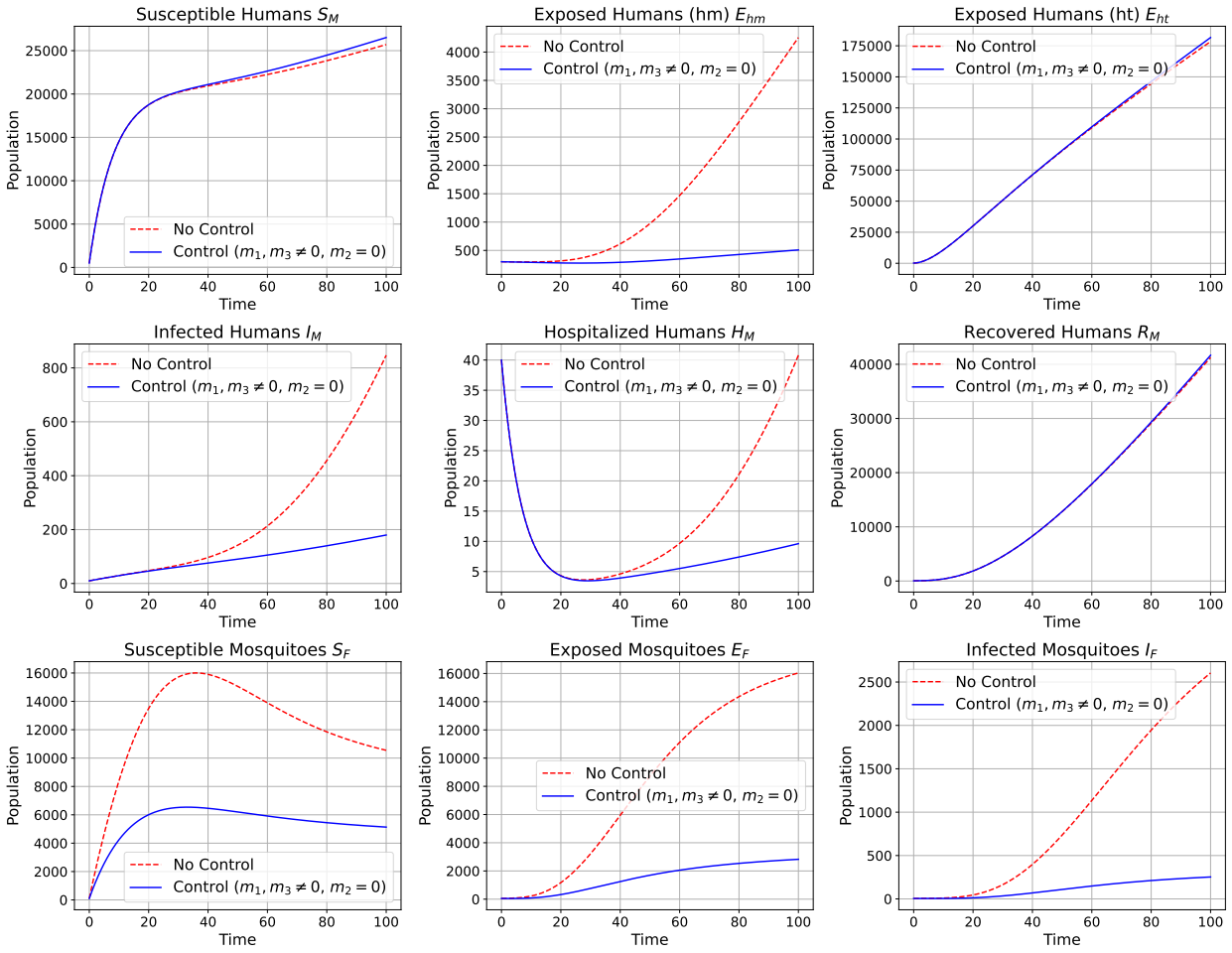

Figure 9: *Optimal bed-nets and insecticide spray control strategy.*

6.3.4. Optimal Bed-nets & Medication

This strategy combines treated bed-nets (m_1) and medication (m_2) controls, without insecticide spray ($m_3 = 0$). Figure 10 illustrates a marked reduction in infected humans, with increased effectiveness after ten days. It also shows declines in susceptible, exposed, and infected mosquito populations.

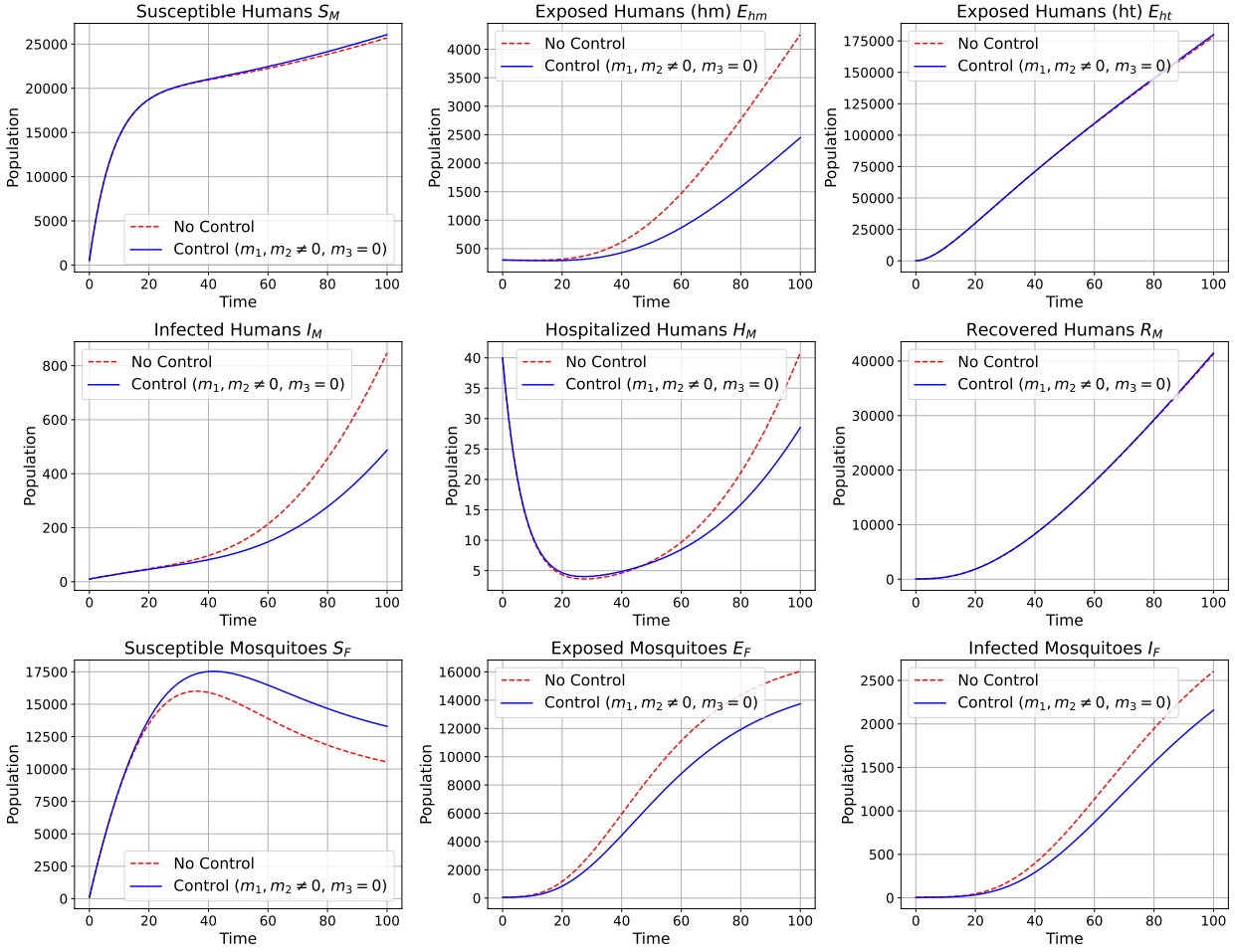

Figure 10: *Optimal bed-nets and medication control strategy.*

7. Spatial Model Implementation

We extended the classical malaria transmission model into a spatial framework by dividing the study area into a 10×10 grid of patches, each with its own human and mosquito compartments. Within each patch, human classes (S_M, E_{hm}, E_{ht}, I_M, H_M, R_M) and mosquito classes (S_F, E_F, I_F) were modeled using coupled ordinary differential equations. Mosquito dispersal between adjacent patches was represented as a diffusion process, allowing movement to four nearest neighbors at a fixed rate. Human movement was not included. The system was solved numerically using the `odeint` solver over 50 time units, with infection seeded in the central patch. The figure 11 displays heatmaps of infected humans (I_M) across the grid at six time points. Initially, infection is localized centrally, then spreads outward symmetrically due to mosquito movement and local transmission. Darker red indicates higher infection levels. A consistent color scale allows comparison across times. This illustrates how spatial processes shape malaria dynamics and highlights the importance of spatial heterogeneity for understanding and controlling transmission.

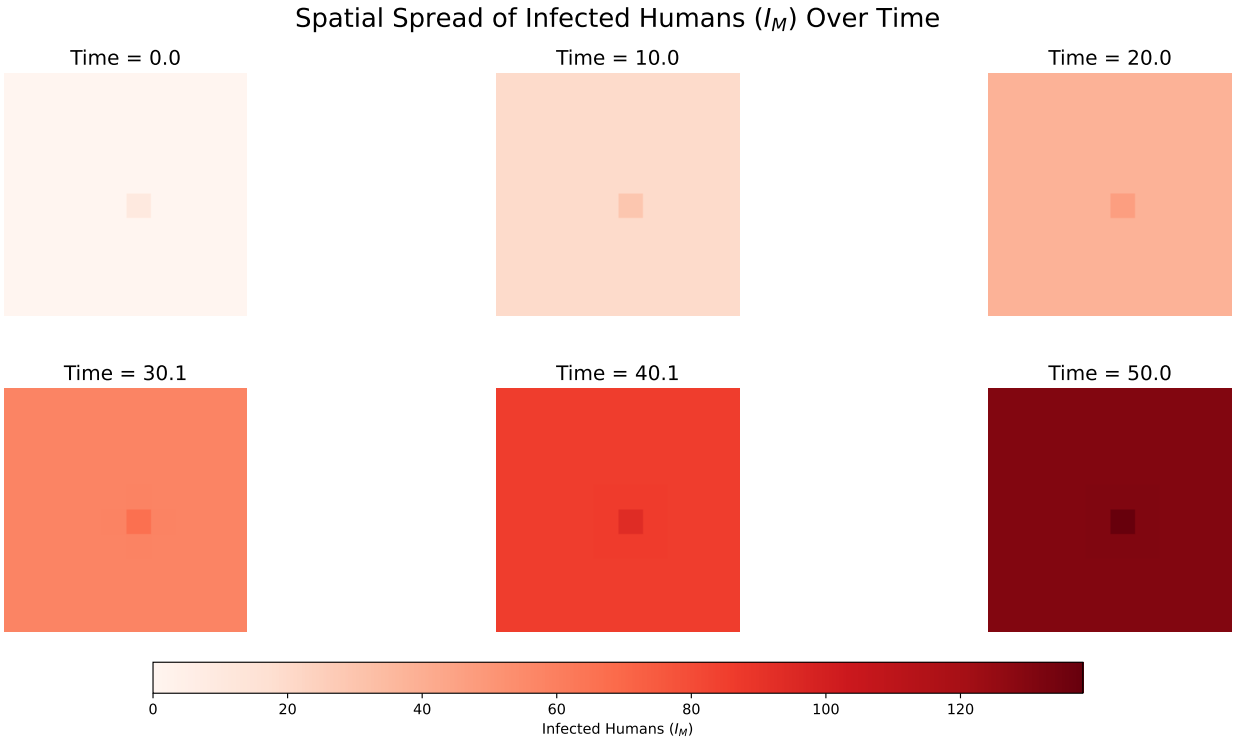

Figure 11: *Spatial spread of infected humans (I_M) across a 10×10 grid at six time points*

Table 2: *Parameters Description*

Parameters	Values	Sources
λ_M	2500	[52]
β_F	0.8333	[52]
β_M	0.022	[52]
η_M	0.0083	assumed
ω_M	0.021	assumed
α_M	18	[52]
γ_M	0.123	assumed
ϵ_M	0.00004212	[52]
ψ_M	0.045	[52]
ρ_M	0.0083	[52]
ϕ_M	0.0071	assumed
μ_M	0.0000345	[52]
δ_M	0.1429	assumed
λ_F	1000	[52]
ϵ_F	0.033	[52]
ϕ_F	0.083	[52]

8. Discussion

Malaria remains one of the most serious infectious diseases worldwide, caused by the protozoan *Plasmodium* and transmitted via bites from female *Anopheles* mosquitoes. Understanding the transmission dynamics is vital for developing effective control strategies. In this study, we constructed a deterministic compartmental model, denoted as $S_M E_{hm} E_{ht} I_M H_M R_M - S_F E_F I_F$, to represent the complex interactions between human and mosquito populations.
A primary focus of our analysis is the stability of the malaria-free equilibrium. Sensitivity analysis of the basic reproduction number R_0 revealed key parameters influencing disease transmission, such as the mosquito biting rate α_M and the transmission probability from humans to mosquitoes β_F (see Figures 12 and 13). These findings corroborate previous research emphasizing the importance of vector-host contact rates and transmission probabilities in malaria dynamics [1–3]. Moreover, we formulated an optimal control problem based on Pontryagin's Maximum Principle, incorporating three intervention strategies aimed at reducing the disease burden.

(i) Use of insecticide-treated bed nets (m_1),

(ii) Medication treatment of infected individuals (m_2),

(iii) Insecticide spraying to reduce mosquito populations (m_3).

Given results demonstrate that the combined application of all three controls is more effective in reducing malaria transmission than any single strategy alone. Among individual measures, the use of bed nets (m_1) is particularly impactful, as it provides a physical barrier that significantly reduces human exposure to infectious mosquito bites. Consistent and widespread use of bed nets, especially when integrated with other interventions, offers a promising approach to malaria control.

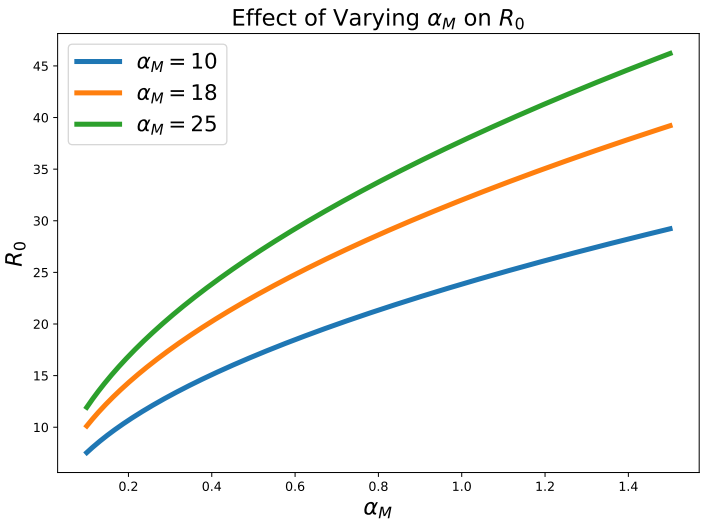

Figure 12: *Effect of varying mosquito biting rate* α_M *on the basic reproduction number* R_0.

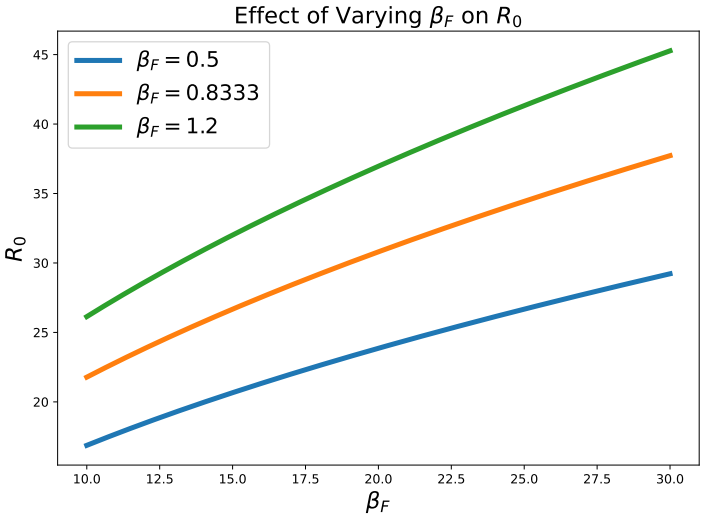

Figure 13: *Effect of varying transmission probability from humans to mosquitoes β_F on the basic reproduction number R_0.*

These insights are consistent with the broader literature, which emphasizes that maintaining $R_0 < 1$ through targeted interventions is essential for malaria elimination [3, 6, 7]. Future work could extend this model by incorporating spatial heterogeneity and stochastic effects to better capture real-world complexities.

9. Conclusion

In this research, we developed a comprehensive mathematical model to simulate malaria transmission dynamics by incorporating both homogeneous and heterogeneous exposed human compartments through a system of nonlinear differential equations. We derived the basic reproduction number R_0 and performed a detailed sensitivity analysis, identifying key parameters such as the mosquito biting rate α_M and the transmission probability β_M as the most influential factors driving disease spread. To mitigate malaria transmission, we formulated an optimal control problem using Pontryagin's Maximum Principle, introducing three time-dependent control strategies: use of treated bed nets (m_1), medical treatment (m_2), and insecticide spraying (m_3). Our innovative approach explored the combined effects of two strategies while gradually reducing the third, offering valuable insights into the trade-offs involved in malaria control planning. The resulting optimal control profiles exhibited increasing trends across all three interventions. Numerical simulations confirmed that integrating multiple interventions yields the most substantial reduction in malaria transmission. Specifically, the combined application of treated bed nets, medication, and insecticide spraying proved to be the most effective strategy. These findings are consistent with existing literature emphasizing the importance of integrated vector management and coordinated preventive and treatment measures to reduce the malaria burden. This study underscores the value of integrative mathematical modeling in guiding evidence-based public health interventions for malaria control and highlights the critical role of targeting vector-host interactions and key transmission parameters to achieve disease reduction and eventual elimination. Future research can further enhance

this framework by incorporating spatial heterogeneity to capture regional variations in transmission intensity, stochastic effects to reflect environmental and demographic uncertainties, and additional interventions such as vaccination or genetic vector control technologies. Moreover, coupling the model with real-time epidemiological and climatic data through data assimilation techniques can improve predictive accuracy and inform adaptive policy decisions in malaria-endemic regions.

Data Availability
No data availability

Conflict of Interest
The authors declare that there is no conflict of interest.

Funding
No funds.

Acknowledgements

Authors (Dr. Nadeem Abbas and Prof. Dr. Wasfi Shatanawi) would like to thank Prince Sultan University for their support through the TAS research lab.

References

[1] Hanif Ullah, Muhammad Inayatullah Khan, Nehaz Muhammad Suleman, Nayab Ismail, Zahid Khan, and Ghalib Sayyid. A review on malarial parasite. *World Journal of Zoology*, 10(4):285–290, 2015.

[2] Noppadon Tangpukdee, Chatnapa Duangdee, Polrat Wilairatana, and Srivicha Krudsood. Malaria diagnosis: a brief review. *The Korean journal of parasitology*, 47(2):93, 2009.

[3] Centers for Disease Control and Prevention Malaria. About malaria. `https://www.cdc.gov/malaria/about/faqs.html`, 2022. Accessed October 13 2022.

[4] Zhenbu Zhang and Tor A Kwembe. Qualitative analysis of a mathematical model for malaria transmission and its variation. 23:195–210, 2016.

[5] World Health Organization. *WHO Malaria Policy Advisory Group (MPAG) meeting, October 2022*. World Health Organization, 2022.

[6] Sandip Mandal, Ram Rup Sarkar, and Somdatta Sinha. Mathematical models of malaria-a review. *Malaria journal*, 10(1):202, 2011.

[7] Ronald Ross. *The prevention of malaria*. John Murray, 1911.

[8] Gideon A Ngwa and William S Shu. A mathematical model for endemic malaria with variable human and mosquito populations. *Mathematical and computer modelling*, 32(7-8):747–763, 2000.

[9] Francis T Oduro, Gabriel A Okyere, and George Theodore Azu-Tungmah. Transmission dynamics of malaria in ghana. *Journal of Mathematics research*, 4(6):22, 2012.

[10] Abadi Abay Gebremeskel and Harald Elias Krogstad. Mathematical modelling of endemic malaria transmission. *American Journal of Applied Mathematics*, 3(2):36–46, 2015.

[11] Julius Tumwiine, JYT Mugisha, and Livingstone S Luboobi. A mathematical model for the dynamics of malaria in a human host and mosquito vector with temporary immunity. *Applied mathematics and computation*, 189(2):1953–1965, 2007.

[12] Egide Ndamuzi and Paterne Gahungu. Mathematical modeling of malaria transmission dynamics: case of burundi. 2021.

[13] Mohammed S Abdo, Mohammed Amood AL Kamarany, Khaled Ahmed Suhail, and Ahmed Suliman Majam. Vaccination-based measles outbreak model with fractional dynamics. *Abhath Journal of Basic and Applied Sciences*, 1(2):6–10, 2022.

[14] Hyun M Yang and Marcelo U Ferreira. Assessing the effects of global warming and local social and economic conditions on the malaria transmission. *Revista de saude publica*, 34:214–222, 2000.

[15] Hyun M Yang. A mathematical model for malaria transmission relating global warming and local socioeconomic conditions. *Revista de saude publica*, 35:224–231, 2001.

[16] Dereje Gutema Edossa and Purnachandra Rao Koya. Mathematical modeling the dynamics of endemic malaria transmission with control measures. *IOSR Journal of Mathematics (IOSR-JM)*, 15(4):25–41, 2019.

[17] OC Collins and KJ Duffy. A mathematical model for the dynamics and control of malaria in nigeria. *Infectious disease modelling*, 7(4):728–741, 2022.

[18] Agnes Adom-Konadu, Ernest Yankson, Samuel M Naandam, and Duah Dwomoh. A mathematical model for effective control and possible eradication of malaria. *Journal of Mathematics*, 2022(1):6165581, 2022.

[19] Abid Ali Lashari, Shaban Aly, Khalid Hattaf, Gul Zaman, Il Hyo Jung, and Xue-Zhi Li. Presentation of malaria epidemics using multiple optimal controls. *Journal of Applied mathematics*, 2012(1):946504, 2012.

[20] Mayowa M Ojo. Mathematical modeling of malaria disease with control strategy. *Communications in mathematical biology and neuroscience*, 2020.

[21] Ousmane Koutou, Bakary Traoré, and Boureima Sangaré. Mathematical modeling of malaria transmission global dynamics: taking into account the immature stages of the vectors. *Advances in Difference Equations*, 2018(1):220, 2018.

[22] Yves Tinda Mangongo, Joseph-Désiré Kyemba Bukweli, Justin Dupar Busili Kampempe, Rostin Matendo Mabela, and Justin Manango Wazute Munganga. Stability and global sensitivity analysis of the transmission dynamics of malaria with relapse and ignorant infected humans. *Physica Scripta*, 97(2):024002, 2022.

[23] Temesgen Duressa Keno, Lemessa Bedjisa Dano, and Oluwole Daniel Makinde. Modeling and optimal control analysis for malaria transmission with role of climate variability. *Computational and Mathematical Methods*, 2022(1):9667396, 2022.

[24] Syeda Alishwa Zanib, Sehrish Ramzan, Nadeem Abbas, Aqsa Nazir, and Wasfi Shatanawi. Comprehensive analysis of conformable mathematical model of ebola virus with effective control strategies. *Scientia Iranica*, 2024.

[25] Sehrish Ramzan, Syeda Alishwa Zanib, Sadia Yasin, and Muzamil Abbas Shah. A fractional calculus approach to smoking dynamics with bifurcation analysis. *Modeling Earth Systems and Environment*, 10(5):5851–5869, 2024.

[26] Eyup Cetin, Serap Kiremitci, and Baris Kiremitci. Developing optimal policies to fight pan-

demics and covid-19 combat in the united states. *European Journal of Pure and Applied Mathematics*, 13(2):369–389, 2020.

[27] Muhammad Shoaib Arif, Kamaleldin Abodayeh, and Yasir Nawaz. A computational scheme for stochastic non-newtonian mixed convection nanofluid flow over oscillatory sheet. *Energies*, 16(5):2298, 2023.

[28] Mukhtiar Khan, Nadeem Khan, Ibad Ullah, Kamal Shah, Thabet Abdeljawad, and Bahaaeldin Abdalla. A novel fractal fractional mathematical model for hiv/aids transmission stability and sensitivity with numerical analysis. *Scientific Reports*, 15(1):9291, 2025.

[29] Yasir Nawaz, Muhammad Shoaib Arif, and Kamaleldin Abodayeh. Predictor–corrector scheme for electrical magnetohydrodynamic (mhd) casson nanofluid flow: a computational study. *Applied Sciences*, 13(2):1209, 2023.

[30] Syeda Alishwa Zanib and Muzamil Abbas Shah. A piecewise nonlinear fractional-order analysis of tumor dynamics: Estrogen effects and sensitivity. *Modeling Earth Systems and Environment*, 10(5):6155–6172, 2024.

[31] Yasir Nawaz, Muhammad Shoaib Arif, Kamaleldin Abodayeh, Muhammad Usman Ashraf, and Mehvish Naz. A new explicit numerical scheme for enhancement of heat transfer in sakiadis flow of micro polar fluid using electric field. *Heliyon*, 9(10), 2023.

[32] Syeda Alishwa Zanib, Sehrish Ramzan, Muzamil Abbas Shah, Nadeem Abbas, and Wasfi Shatanawi. Comprehensive analysis of mathematical model of hiv/aids incorporating fisherfolk community. *Modeling Earth Systems and Environment*, 10(5):6323–6340, 2024.

[33] SY Tchoumi, ML Diagne, H Rwezaura, and JM Tchuenche. Malaria and covid-19 co-dynamics: A mathematical model and optimal control. *Applied mathematical modelling*, 99:294–327, 2021.

[34] Muhammad Sinan, Hijaz Ahmad, Zubair Ahmad, Jamel Baili, Saqib Murtaza, MA Aiyashi, and Thongchai Botmart. Fractional mathematical modeling of malaria disease with treatment & insecticides. *Results in Physics*, 34:105220, 2022.

[35] Mohamed Salah Alhaj. Mathematical model for malaria disease transmission. *Journal of Mathematical Analysis and Modeling*, 4(1):1–16, 2023.

[36] AS Alqahtani, Sehrish Ramzan, Syeda Alishwa Zanib, Aqsa Nazir, Khalid Masood, and MY Malik. Mathematical modeling and simulation for malaria disease transmission using the cf fractional derivative. *Alexandria Engineering Journal*, 101:193–204, 2024.

[37] Pride Duve, Samuel Charles, Justin Munyakazi, Renke Lühken, and Peter Witbooi. A mathematical model for malaria disease dynamics with vaccination and infected immigrants. *Math. Biosci. Eng*, 21(1):1082–1109, 2024.

[38] AL Olutimo, NU Mbah, FA Abass, and AA Adeyanju. Effect of environmental immunity on mathematical modeling of malaria transmission between vector and host population. *Journal of Applied Sciences and Environmental Management*, 28(1):205–212, 2024.

[39] Ayman Hussein Alfeel, Tagwa Yousif Elsayed Yousif, Ammar Abdelmola, Praveen Kumar, Hussam Ali Osman, Rabab Hassan Elshaikh, Muhammad Saboor, Salah Omar Hussein, Elryah I Ali, and Izzeldin Elbashir. Prevalence and demographic analysis of hemoglobinopathies in newborns: A three-year study at thumbay teaching hospital, ajman-uae. *Journal of Blood Medicine*, pages 123–134, 2025.

[40] Pauline Van den Driessche and James Watmough. Reproduction numbers and sub-threshold endemic equilibria for compartmental models of disease transmission. *Mathematical biosciences*, 180(1-2):29–48, 2002.

[41] Carlos Castillo-Chavez, Zhilan Feng, Wenzhang Huang, et al. On the computation of r (o)

and its role on global stability. 2001.

[42] A Fall, Abderrahman Iggidr, Gauthier Sallet, and Jean-Jules Tewa. Epidemiological models and lyapunov functions. *Mathematical Modelling of Natural Phenomena*, 2(1):62–83, 2007.

[43] Sally M Blower and Hadi Dowlatabadi. Sensitivity and uncertainty analysis of complex models of disease transmission: an hiv model, as an example. *International Statistical Review/Revue Internationale de Statistique*, pages 229–243, 1994.

[44] Sally M Blower, Diana Hartel, Hadi Dowlatabadi, Robert M Anderson, and Roy M May. Drugs, sex and hiv: a mathematical model for new york city. *Philosophical Transactions of the Royal Society of London. Series B: Biological Sciences*, 331(1260):171–187, 1991.

[45] Alexander Hoare, David G Regan, and David P Wilson. Sampling and sensitivity analyses tools (sasat) for computational modelling. *Theoretical Biology and Medical Modelling*, 5(1):4, 2008.

[46] Laura Nyawira Wangai, Muriira Geoffrey Karau, Paul Nthakanio Njiruh, Omar Sabah, Francis Thuo Kimani, Gabriel Magoma, and Njagi Kiambo. Sensitivity of microscopy compared to molecular diagnosis of p. falciparum: implications on malaria treatment in epidemic areas in kenya. *African journal of infectious diseases*, 5(1), 2011.

[47] Getachew Teshome Tilahun, Oluwole Daniel Makinde, and David Malonza. Modelling and optimal control of typhoid fever disease with cost-effective strategies. *Computational and mathematical methods in medicine*, 2017(1):2324518, 2017.

[48] Getachew Teshome Tilahun, Oluwole Daniel Makinde, and David Malonza. Modelling and optimal control of typhoid fever disease with cost-effective strategies. *Computational and mathematical methods in medicine*, 2017(1):2324518, 2017.

[49] Lev Semenovich Pontryagin. *Mathematical theory of optimal processes*. Routledge, 2018.

[50] K Renee Fister, Suzanne Lenhart, and Joseph Scott McNally. Optimizing chemotherapy in an hiv model. 1998.

[51] John C Butcher. On the implementation of implicit runge-kutta methods. *BIT Numerical Mathematics*, 16(3):237–240, 1976.

[52] Nakul Rashmin Chitnis. *Using mathematical models in controlling the spread of malaria*. PhD thesis, 2005.